AD-A140 611 MATERIALS RESEARCH FOR ADVANCED INERTIAL INSTRUMENTATION TASK 3 RARE EART.. (U) CHARLES STARK DRAPER LAB INC CAMBRIDGE MA K KUMAR ET AL. FEB 84 1/1

UNCLASSIFIED CSDL-R-1695 N00014-77-C-0388 F/G 20/3 NL

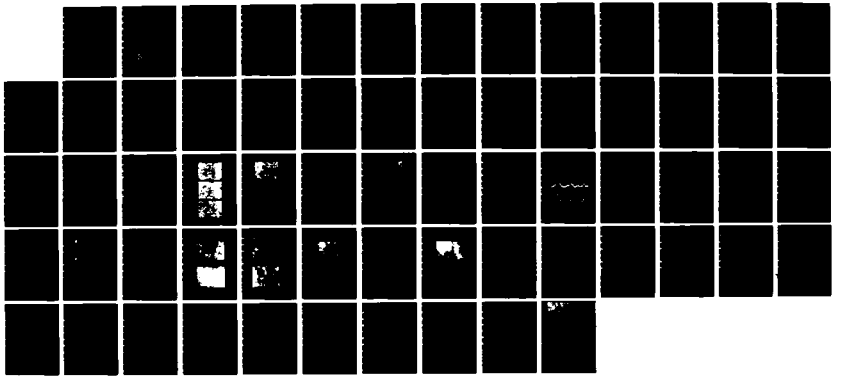

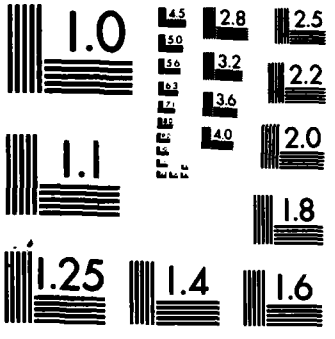

CSDL-R-1695

MATERIALS RESEARCH FOR ADVANCED INERTIAL INSTRUMENTATION

TASK 3: RARE EARTH MAGNETIC MATERIAL TECHNOLOGY AS RELATED TO GYRO TORQUERS AND MOTORS

FEBRUARY 1984

FINAL REPORT

by

K. KUMAR, D. DAS, H. NEWBORN

Prepared for the Office of Naval Research, Department of the Navy, under Contract N00014-77-C-0388

The Charles Stark Draper Laboratory, Inc.
Cambridge, Massachusetts 02139

UNCLASSIFIED

SECURITY CLASSIFICATION OF THIS PAGE *(When Data Entered)*

REPORT DOCUMENTATION PAGE

READ INSTRUCTIONS BEFORE COMPLETING FORM

1. REPORT NUMBER: CSDL-R-1695	2. GOVT ACCESSION NO.: AD-A140677
3. RECIPIENT'S CATALOG NUMBER:	
4. TITLE *(and Subtitle)*: MATERIALS RESEARCH FOR ADVANCED INERTIAL INSTRUMENTATION; TASK 3: RARE EARTH MAGNETIC MATERIAL TECHNOLOGY AS RELATED TO GYRO TORQUERS AND MOTORS	5. TYPE OF REPORT & PERIOD COVERED: FINAL REPORT 10/1/77-12/31/83
	6. PERFORMING ORG. REPORT NUMBER:
7. AUTHOR(s): K. Kumar, D. Das, and H. Newborn	8. CONTRACT OR GRANT NUMBER(s): N00014-77-C-0388
9. PERFORMING ORGANIZATION NAME AND ADDRESS: The Charles Stark Draper Laboratory, Inc. 555 Technology Square Cambridge, Massachusetts 02139	10. PROGRAM ELEMENT, PROJECT, TASK AREA & WORK UNIT NUMBERS:
11. CONTROLLING OFFICE NAME AND ADDRESS: Office of Naval Research Department of the Navy 800 N. Quincy St., Arlington, Virginia 20217	12. REPORT DATE: February 1984
	13. NUMBER OF PAGES: 64
14. MONITORING AGENCY NAME & ADDRESS *(if different from Controlling Office)*:	15. SECURITY CLASS. *(of this report)*: Unclassified
	15a. DECLASSIFICATION/DOWNGRADING SCHEDULE:

16. DISTRIBUTION STATEMENT *(of this Report)*

Approved for public release; distribution unlimited

17. DISTRIBUTION STATEMENT *(of the abstract entered in Block 20, if different from Report)*

18. SUPPLEMENTARY NOTES

19. KEY WORDS *Continue on reverse side if necessary and identify by block number)*

$SmCo_5$ Magnets	Sintering	Flux Stability
Sm_2Co_{17} Magnets	Temperature Compensated Magnets	
Hot Isostatic Pressing	Thermal Expansion Coefficient	
Arc Plasma Spraying	Permanent Magnets	

20. ABSTRACT *(Continue on reverse side if necessary and identify by block number)*

The initial objectives of this effort included development of the appropriate understanding (and demonstration of the feasibility) of being able to produce high energy product $SmCo_5$ magnets with (1) high flux stability, (2) adequate temperature compensation, and (3) coefficient of thermal expansion matched closely to that of beryllium. The first objective was the most difficult to achieve and required the most effort. The third proved to be the least problematic.

(OVER)

DD FORM 1 JAN 73 1473 EDITION OF 1 NOV 65 IS OBSOLETE

UNCLASSIFIED

SECURITY CLASSIFICATION OF THIS PAGE *(When Data Entered)*

The approach that was initially adopted concentrated on producing magnets with high flux stability by improving the conventional sintering process to minimize contamination from the environment. This effort resulted in magnets with extremely high H_{ci} and H_k values (of 50 and 33.5 kOe respectively). Even though an improved flux decay rate of 280 ppm/decade was measured in magnets fabricated with these procedures (compared to 1000 to 2000 ppm/decade measured for commercial magnets), this value was still larger than that measured earlier for isotropic plasma sprayed $SmCo_5$ magnets. The desire to produce magnets with additional improved flux decay behavior, while retaining the compact alignment capability inherent in the powder metallurgy process (and absent in the then plasma sprayed material), dictated the pursuit of the hot isostatic pressing (HIP) process to achieve the fine grain (and, preferably, low-oxygen-containing) microstructures, typical of thermally optimized plasma sprayed material. HIP was developed with considerable success and magnets with magnetic properties comparable to those of sintered magnets were produced. The HIP magnets, like the fine-grain plasma sprayed material produced earlier, showed an absence of internal microcracks (which are present in conventionally produced magnets) and could be produced with lower oxygen levels by appropriate selection of coarse powder sizes for alignment and consolidation. Because the HIP technique that was developed was somewhat more expensive than conventional sintering, plasma spraying investigations were incorporated later into this program as a lower cost alternative. The objective of the plasma spraying activity consisted of achieving high energy product through either shifting the $SmCo_5$ composition to Sm_2Co_{17} or, more desirably, producing textured deposits with the hexagonal C-axis normal to the plane of deposition.

Considerable successes were achieved during the course of this activity. The lowest flux decay rate measured for a HIP magnet was 43 ppm/decade. This was also the lowest measured for $SmCo_5$ magnets at this laboratory. These studies showed that, contrary to widely accepted belief, the values of H_{ci} and H_k had little bearing on the flux decay rate, which was directly related to the magnet composition and its prior thermal processing. These findings provided, for the first time, the recipe for fabricating magnets with high flux stability. Use of HIP as the fabrication technology also permitted the fabrication of high energy product, full-circle radial orientation ring magnets, which were hitherto unavailable. These ring magnets found significant application in novel device designs. Erbium-containing temperature compensated magnets were produced with the maximum (achieved) energy product value of about 11.6 MGOe. Quite significantly, it was demonstrated that the desired C-axis orientation, normal to the deposition plane, was achievable in sprayed $SmCo_5$ deposits. The coercivities of these deposits were less than needed and this precluded the fabrication of sprayed magnets with high values of the energy product. The work that was performed, however, appeared to indicate that additional work could lead to the production of good quality magnets with this technique.

CSDL-R-1695

MATERIALS RESEARCH FOR ADVANCED INERTIAL INSTRUMENTATION

TASK 3: RARE EARTH MAGNETIC MATERIAL TECHNOLOGY AS RELATED TO GYRO TORQUERS AND MOTORS

FINAL REPORT

February 1984

by

K. Kumar, D. Das, H. Newborn*

Approved: 

M. S. Sapuppo, Head
Instrument Development
Department

Prepared for the Office of Naval Research
Department of the Navy, Under Contract N00014-77-C-0388

The Charles Stark Draper Laboratory, Inc.
Cambridge, Massachusetts 02139

*Some of the work described in this report was performed at the Francis Bitter National Magnet Laboratory by the authors as visiting scientists.

ACKNOWLEDGEMENTS

We wish to express our appreciation to the Francis Bitter National Magnet Laboratory, MIT, for their assistance in making the high-field magnets available for our studies in this program. Our sincere thanks to C.R. Dauwalter for carrying out the flux stability measurements.

This report was prepared by The Charles Stark Draper Laboratory, Inc., under Contract N00014-77-C-0388 with the Office of Naval Research of the Department of the Navy.

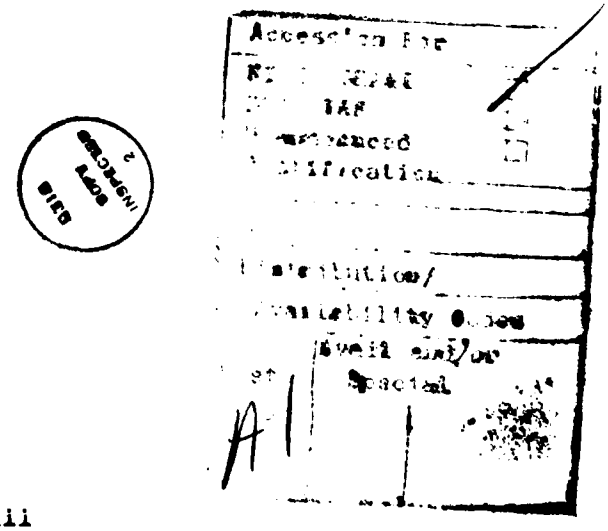

TABLE OF CONTENTS

LIST OF ILLUSTRATIONS

LIST OF TABLES

SECTION 1

INTRODUCTION

1.1 Program Background

The Charles Stark Draper Laboratory, Inc. (CSDL) is involved with research and development in various technologies related to guidance and navigation for vehicles of all types. Samarium-cobalt magnets, because of their high values of intrinsic coercivity (H_{ci}) and maximum energy product $(BH)_{max}$, are very attractive permanent magnet materials for applications in inertial instruments. They are used within inertial systems as components of the instruments or sensors - the gyro and accelerometer. The lower volume of the Sm-Co magnet impacts favorably on the overall size and weight of the instrument.

In addition to high energy product, magnets used in advanced inertial instruments must also possess long-term flux stability, insensitivity to minor temperature variations, and physical properties compatible with those of beryllium. (Beryllium is the structural material used in modern inertial instruments.) Commercially available $SmCo_5$ magnets, produced by the state-of-the-art powder metallurgy process, possess more than adequate H_{ci} and $(BH)_{max}$, and the thermal expansion coefficient requires only a small amount of tailoring to match that of beryllium. The two important areas where the commercial $SmCo_5$ magnets fail to meet the requirements of advanced inertial instruments are: (1) lack of adequate, and predictable flux stability and (2) large variation of flux associated with a small temperature change.

Under sponsorship from the Office of Naval Research a comprehensive research program was initiated at CSDL in October 1977 with the aim of utilizing improved $SmCo_5$ magnet fabrication procedures to achieve the goals of high flux stability, temperature compensation, and thermal expansion matched to that of beryllium. During the first two years of

the present program, efforts focused on sintered and hot isostatically pressed magnets of the $SmCo_5$ composition. A new subtask was added as of October 1979, which concentrated on Sm-Co magnets fabricated by the arc-plasma-spray (APS) process. The motivation behind this subtask was the earlier achievement of outstanding success with near-isotropic $SmCo_5$ magnets using this process at CSDL.

1.2 Objectives

The objectives of the present program were (1) to investigate the arc-plasma-spray process for fabricating high energy product Sm-Co magnets, and (2) to develop improved powder metallurgical procedures to produce inertial-grade $SmCo_5$ magnets that would provide improvements in the following areas:

(1) Long-term flux stability at constant temperature (140°F)

Desired:	0.008 ppm/90-day
Available	Sintered: ~1 ppm/day
	Plasma Sprayed: 0.05 ppm/day

(2) Thermal stability of residual induction

Desired:	0.1 ppm/°F
Available	300 ppm/°F

(3) Tailoring of thermal expansion coefficient

Desired, same as beryllium:	6.6 μin./in. °F
Available:	
Isotropic:	4.7 μin./in. °F
Anisotropic:	
(a) Along magnetization direction:	3.1 μin./in. °F
(b) Normal to magnetization direction:	7.1 μin./in. °F

SECTION 2

RATIONALE AND APPROACH

2.1 Flux Stability at Constant Temperature

Of the three objectives listed in the previous section, the first was the most important and required a careful analysis of theory and available experimental data to formulate a viable approach.[1]* Based on this analysis it was concluded that improvements needed to be effected in both the intrinsic coercivity and the general characteristics (with respect to loop squareness) of the second quadrant (of the $4\pi M$ vs. H curve). In order to obtain the desired magnetic behaviors, the structural requirements from the materials point of view included fabrication of highly densified (93 percent of theoretical or better) sintered bodies comprised of very fine crystallites with the fewest number of defects possible.

The anisotropy magnetic field of the compound $SmCo_5$ is about 350 kOe. The hexagonal $SmCo_5$ crystal reaches its saturation magnetization (of about 10 kG) when a magnetic field of roughly 10 kOe intensity is applied along its easy magnetization direction, which is the C-axis of the crystal. In order to reach saturation along the hard basal plane direction, however, a field of about 350 kOe is required to achieve a similar result. The physical implication of the foregoing is that a single domain $SmCo_5$ particle [smaller than 1.6 μm in any direction[2]] containing zero defects would theoretically require a reverse magnetic field of 350 kOe to completely reverse its magnetization. In other words, the expected intrinsic coercivity of such a particle would be 350 kOe. A magnet body composed of such

* Superscript numerals refer to similarly numbered items in the List of References.

densely packed defect-free particles would, therefore, have a residual induction (B_R) of 10 kG, H_{ci} of 350 kOe, a $(BH)_{max}$ of 25 MGOe, and an absolutely perfect rectangular hysteresis loop of gigantic proportions.

The demagnetization process in sintered Sm-Co magnets does not appear to result from the vector rotation of magnetization. If it were a rotational process, the intrinsic coercivity would be 350 kOe instead of only 15 to 30 kOe (which is generally found for commercial magnets). The mechanism of demagnetization has been shown to include nucleation and growth of reverse domains under the influence of reverse (applied) magnetic fields. The nucleation of such reverse domains occurs at defect sites in the crystallite. Once the nucleated domain reaches a critical size, it sweeps easily across the entire grain with little or no required increase in the intensity of the applied reverse field. The magnitude of the reverse field required for complete reversal of magnetization can vary from very small (self-demagnetizing field) to very high (many decades of kOe field) intensity. A magnet body comprised of millions of crystallites would therefore demagnetize over a wide range of applied field. The larger the number of defects in a crystal, the more likely it is to reverse at a lower field. A magnet that has a lower coercivity than another must therefore have more defects per crystal. Magnets with larger grain sizes are expected to have more defects per crystal and therefore should, and do, have lower coercivity.

Earlier work[3,4] had reported that coercivity is related to the long-term flux stability of a magnet. And from the reasons given above, coercivity is seen to be directly related to the number of defects per crystal. With a given number of defects per unit volume of a magnet it therefore appears desirable to have the grain size as small as possible to obtain fewer defects per crystal. Thus, one of the two structural requirements for obtaining a more stable magnet is that the grain size in the magnet must be as small as possible.

The discussion, so far, has dealt with the reversal of magnetization initiated at defects present in the magnets. There are a number of such defects, but the ones that are known to be the most significant contributors are related to the presence of foreign atoms in the alloy. Two important sources of contamination by foreign atoms are (1) reaction with crucibles (used for melting the alloys), and (2) contamination by oxygen in the air (which invariably comes in contact with the alloy and its powder during processing). Since the alloy must be prepared by melting samarium and cobalt together, some contamination inevitably results from the crucible walls. This can be minimized by proper melting procedures. The amount of oxygen pickup during processing can also be controlled to a certain extent, but it is nearly impossible to completely eliminate it. (Commercial sintered magnets contain between one and two weight-percent oxygen.)

Research recently conducted with arc-plasma-sprayed magnets at CSDL provided strong evidence of the damaging influence of oxygen on the coercivity and the coercivity-retaining ability of Sm-Co magnets. The oxygen content in these arc-plasma-sprayed magnets was less by an order of magnitude than that found in commercial sintered magnets. Sprayed magnets also demonstrated almost twice the coercivity.[5] These magnets were greatly resistant to degradation in H_{ci} from the same thermal processing that is known to be severely detrimental to commercial sintered magnets. This increased coercivity-retaining ability was believed to be directly related to the lesser amount of oxygen in the material.[6] Dissolution and reprecipitation processes involving oxygen are known to result in localized composition inhomogeneities which are composed of low anisotropy (and therefore low coercivity) material.[6,7]

An insight into the effect of oxygen on coercivity of $SmCo_5$ magnets was provided by the work of Bartlett and Jorgensen.[7] This work dealt with an analysis of microstructural changes in $SmCo_5$ magnets arising from the incorporation of oxygen during processing of these materials. The excess solubility of oxygen in $SmCo_5$ at 1100°C (which is

close to the sintering temperature) over that at 800°C was shown to be 0.35 to 0.4 percent by weight. As a result, when the oxygen-contaminated magnet is cooled from the sintering temperature, submicron-sized particles of Sm_2O_3 precipitate within the $SmCo_5$ grain and this is accompanied by a depletion of samarium in the surrounding regions. The depleted regions form Sm_2Co_{17} particles which are of much lower anisotropy than $SmCo_5$. In light of these investigations, the variation in coercivity observed by many workers[8-13] can be explained as resulting directly from the oxygen dissolution and precipitation processes in $SmCo_5$. The second important structural requirement, therefore, consisted of achieving a reduction of defects in the $SmCo_5$ crystallites by minimizing the amount of oxygen that was incorporated.

A third obvious requirement for stable performance at constant temperature was the fabrication of a sufficiently densified body whose internal porosity was isolated from the surface. This did not constitute a major concern since practically all sintered Sm-Co magnets meet this density requirement. Normal sintering at over 1100°C produces magnets with density values which are 93 to 95 percent of the theoretical maximum.

2.2 Constant Flux at Varying Temperatures within Small Range

Loss of residual induction of a magnet, resulting from exposure to an elevated temperature below its Curie temperature, is composed of two parts: reversible and irreversible. On cooling down to room temperature, the reversible loss is restored, but the irreversible loss can be regained only by remagnetization, provided there has been no structural change caused by the thermal cycling. With no such structural change, the magnet, (after the first thermal exposure when irreversible losses will occur) will retrace the same induction versus temperature curve on repeated cycling between room temperature and the particular higher temperature to which it was exposed.

$SmCo_5$ shows a continuous decrease of flux at a rate of approximately 400 ppm/°C within the temperature range of room temperature (RT) to 250°C. All light rare earths show a behavior similar to that of samarium. However, the heavier rare earths (HRE) such as erbium (Er), holmium (Ho), dysprosium (Dy), gadolinium (Gd), and terbium (Tb) show an initial increase before they start to decrease towards zero near the Curie temperature.[14,15] Data on the variation of saturation magnetization with temperature for the HRE-Co_5 compounds and the $SmCo_5$ compound over the temperature range of 200°K to 400°K is shown in Figure 1. This set of data was replotted from references 14 and 15. Because of the opposite signs of the temperature coefficients observed between $SmCo_5$ and the HRE Co_5 materials, in this temperature range of interest, a rare-earth composition balanced between samarium and the HREs would be expected to result in near-zero temperature coefficient values.

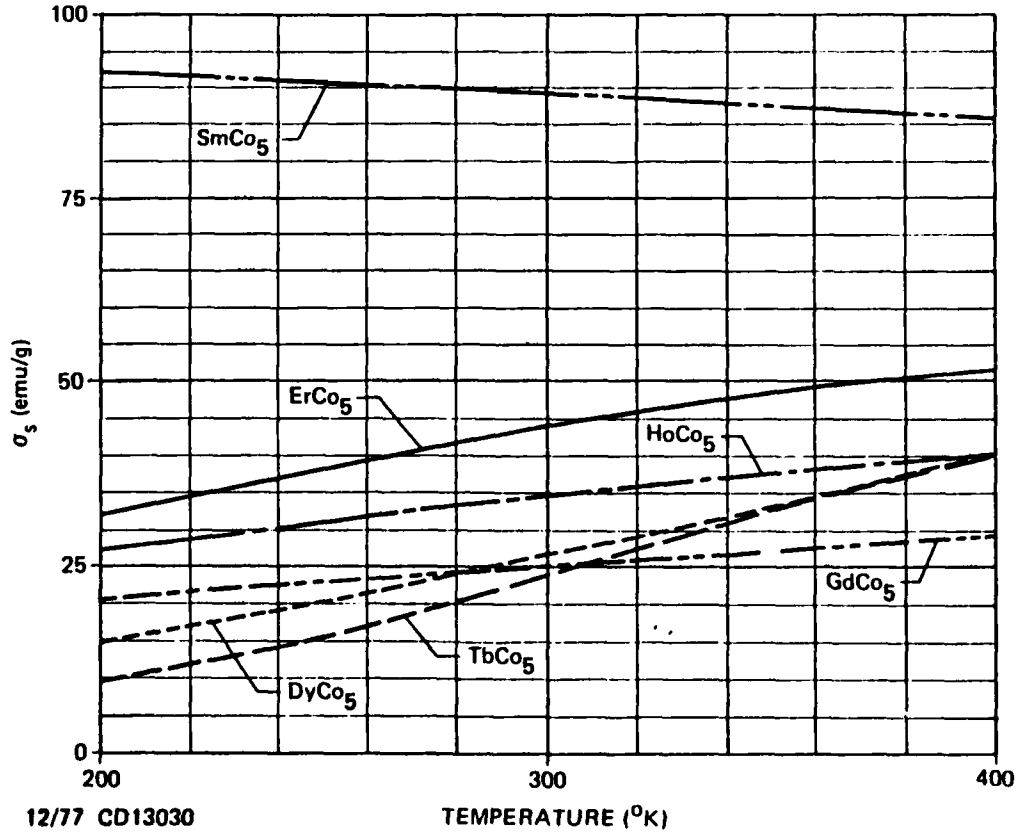

Figure 1. Saturation magnetic moment (σ_s) as a function of temperature of $SmCo_5$ and some HRE Co_5's.

Studies done elsewhere[16,17] have shown the viability of such an approach using the two HRE elements gadolinium and holmium in conjunction with samarium. Approximately 20 percent holmium and 40 percent gadolinium were found to be required to achieve a near-zero temperature coefficient value. The slopes of $TbCo_5$ and $ErCo_5$ are much higher than either $HoCo_5$ or $GdCo_5$. It will therefore require a much smaller amount of $ErCo_5$ or $TbCo_5$ to achieve a similar low (zero) value of the temperature coefficient. The effect of all such substitutions, however, is a reduction in the achieved value of the energy product. It should be noted that almost 50 percent of the energy product is lost when perfect temperature compensation is achieved through the addition of $GdCo_5$. In the case of $HoCo_5$ the loss in energy product would not be expected to exceed about 10 to 15 percent.

2.3 Tailoring of Expansion Coefficient

The thermal expansion coefficient of beryllium is midway between isotropic $SmCo_5$ magnets and the basal plane of the oriented magnet (see Section 1). The expected achievement of a perfect match, therefore, required a reduction in the degree of orientation. The effect of $TbCo_5$ and $ErCo_5$ addition on thermal expansion characteristics, however, needed determination (in the temperature compensated compositions) prior to adjusting the orientation. Unfortunately, the adjustment of thermal expansion was also expected to lead to a reduction in the energy product. This loss would be in addition to the loss in the energy product which is associated with the internal temperature compensation discussed above.

2.4 Arc Plasma Spray Deposition of Sm-Co Magnets

Initial experiments at CSDL showed that sprayed $SmCo_5$ magnets had a remarkably lower rate of flux decay than did the commercial sintered $SmCo_5$ magnets.[18] This was primarily the result of the very high quality of material that had been produced in this program. Sprayed $SmCo_5$ magnets, however, were isotropic, and therefore the energy

product of these magnets was close to half of what is typically obtained in the aligned, commercially fabricated material. To obtain a higher amount of flux from these magnets, one needed to either introduce texture in the deposits or to shift the material composition towards higher cobalt content (by spraying Sm_2Co_{17}-type deposits).

An isotropic Sm_2Co_{17} magnet was expected to show an energy product of about 10 to 12 MGOe as opposed to 7 to 9 MGOe measured in isotropic $SmCo_5$ material and 16 to 18 MGOe found for aligned commercial $SmCo_5$ magnets. An aligned Sm_2Co_{17} magnet would obviously show much higher values. Efforts employing sintering of aligned, binary composition Sm_2Co_{17} magnets were unsuccessful in fabricating magnets with acceptable levels of the intrinsic coercivity (H_{ci}). The maximum value of H_{ci} measured on binary Sm_2Co_{17} sintered material was about 1 to 2 kOe as opposed to a theoretical maximum possibility of about 100 kOe.[19] In contrast, CSDL's sprayed $SmCo_5$ magnets had exhibited coercivities of 68 kOe.[5]

$SmCo_5$ magnets produced by spraying had demonstrated that these magnets could also be cooled slowly from high temperatures, unlike sintered magnets that needed to be cooled rapidly after exposure to high temperature to avoid severe degradation in H_{ci} and second quadrant demagnetization behavior.[6] This degradation was recently shown to result from increased second phase precipitation with decreasing temperatures because of existing chemical inhomogeneities.[20] Slow cooling leads to a decreased amount of strain in the material and therefore a lower incidence of crack formation.[20,21]

The oxygen content of sprayed material is, typically, less than 0.2 weight percent mainly because spraying is conducted in an inert environment chamber and the starting powder (20 to 60 microns) is much larger than that used for sintering (which is less than 10 microns). An added advantage of this process is that while the starting size of the powder particle is large, the average grain size in the deposit is very small. Both amorphous and crystalline $SmCo_5$ material have been produced

using this technique.[22,23] Because of the fine grain size that is obtained, homogenization of the deposit occurs quite readily and very large values of H_{ci} could be obtained by heating the deposited material to temperatures of 850°C to 1000°C. These temperatures were substantially lower than those required for sintering this material.[24,25] This permitted the retention of very fine grain sizes in thermally treated sprayed magnets, on the order of about 2 to 5 microns (compared to 20 to 30 microns in sintered material).[21] All of these factors were believed to have contributed to the high H_{ci} values that were obtained in sprayed $SmCo_5$ material.

The foregoing suggested that it might be possible to obtain reasonably large H_{ci} values in magnets sprayed with Sm_2Co_{17}-type compositions. H_{ci} values obtained in sprayed $SmCo_5$ material were about 20 percent of the anisotropy field. If a similar achievement could be attained in sprayed Sm_2Co_{17} material, coercivities of about 15 to 20 kOe were expected to result from such an effort (which would have been larger than those obtained so far in sintered material by a factor of about 7 to 10). Such an improvement was desirable because it could result in fabrication of sprayed magnets with energy products of about 10 to 12 mGOe and magnets of this type were expected to find several applications. Also, if additional subsequent efforts aimed at developing texture in the $SmCo_5$ and Sm_2Co_{17} materials proved successful, extremely desirable magnets with high magnetic properties would be attained.

SECTION 3

RESULTS AND DISCUSSIONS

3.1 Work Previously Reported

Five interim annual reports[25-29] were submitted, which described the progress in this area for a period of five years, from October 1977 to September 1982. The highlights of the work performed are summarized below.

3.1.1 $SmCo_5$ Magnet Studies by Sintering and Hot Isostatic Pressing

3.1.1.1 Introduction

The most challenging of the three objectives, listed in a previous section, was the achievement of a near-zero flux decay rate; the decay rate of the average commercial $SmCo_5$ magnet was found to be about 2000 ppm/decade of days. Since the coercivity of $SmCo_5$ magnets is much higher than that observed for other permanent magnets, the unusually high decay rates shown by these magnets were difficult to explain. In contrast, the scientific basis for the other two objectives appeared reasonably clear,[16,30] and thus more easily attainable. Early efforts were therefore directed towards attaining lower decay rates and at the same time gaining an understanding of the mechanisms responsible for the unusually high decay rates shown by $SmCo_5$ magnets (produced by conventional powder metallurgy processes).

3.1.1.2 Flux Decay Studies

Since the decay of magnetic induction is a demagnetization process, higher stability was expected to demand a greater resistance to such a process. In turn, this meant that both H_{ci} (the intrinsic

coercivity) and H_k (the reverse field at 90 percent $4\pi M_R$) had to be improved substantially over the state-of-the-art magnets which had H_{ci} in the range of 20 to 30 kOe and H_k of about 5 to 10 kOe; this was despite the fact that these values were already an order of magnitude higher than those of the other permanent magnets known at the time.

In order to achieve this difficult goal, the $SmCo_5$ magnet fabrication technique had to be improved to produce contamination-free magnets, (particularly with respect to oxygen), with fine grain size. The standard sinter technology was improved upon significantly, and this resulted in magnets with outstanding values of coercivity: H_{ci} of approximately 50 kOe and H_k of 33.5 kOe. This led to an observed improvement in the flux decay rate and the value of 280 ppm/decade was measured. In a parallel study, the hot isostatic pressing (HIP) technique was developed for producing $SmCo_5$ magnets. These efforts resulted in more structurally sound magnets with magnetic properties comparable to the sintered variety. The oxygen content of the HIP magnets was about one-half of what was found for sintered magnets. Initial HIPed $SmCo_5$ magnets showed an improved low flux decay rate of 160 ppm/decade. More recent studies of flux decay rates, however, showed that the amount of the second phase, Sm_2Co_7, present in the magnet, played a much more significant role than did the values of H_{ci} and H_k. Larger amounts of this second phase produced a higher rate of decay. Preliminary measurements of flux decay rates of high coercivity and high energy product HIPed $SmCo_5$ magnets showed that the decay rate increased from a low of 43 ppm/decade to a high of 1070 ppm/decade when the nominal samarium content was increased by one weight percent.

In this program, over the past several years, a number of $SmCo_5$ magnets, produced by both sinter and HIP processing, were tested for flux stability. The compositions of these magnets varied between 35.0 and 37.0 weight percent samarium. These were all aged at 900°C for several hours, following the initial high temperature (up to 1100°C+) homogenizing treatments. The homogenized magnets were subjected to

either quick cooling or slow furnace cooling procedures following the 900°C exposure. Examination of the accumulated data provided insight into the nature of the flux decay process in $SmCo_5$ magnets. The decay rates increased with increasing samarium content. Magnets of identical nominal composition showed as much as three to five times higher decay rates when they were quick cooled after the aging treatment, compared to the slow cooled magnets. The densification process (of either sintering or HIP) appeared to have little effect on the decay rates, and, contrary to popular expectation, the decay rates were not dependent on the values of either H_{ci} or H_k. These findings, summarized below, were presented at the 1983 Intermag conference.[31] (Figure 2 gives a graphical depiction of flux decay rate as a function of composition and the rate of cooling from the aging temperature.)

(1) In contrast to earlier reported work, the value of H_k was found to have little bearing on the flux decay rate.

(2) At least two mechanisms appeared to be responsible for the observed flux decay rates:

   (a) The presence and respective amounts of the Sm_2Co_7 phase. The larger the amount, the higher was the decay rate.

   (b) Lowering of dissolved oxygen (and perhaps internal stress to a lesser extent) by slow cooling from aging temperature was found to lower the decay rate.

(3) To maximize stability of magnet flux the material should be composed of near-stoichiometric $SmCo_5$ with low oxygen and possibly a low internal stress.

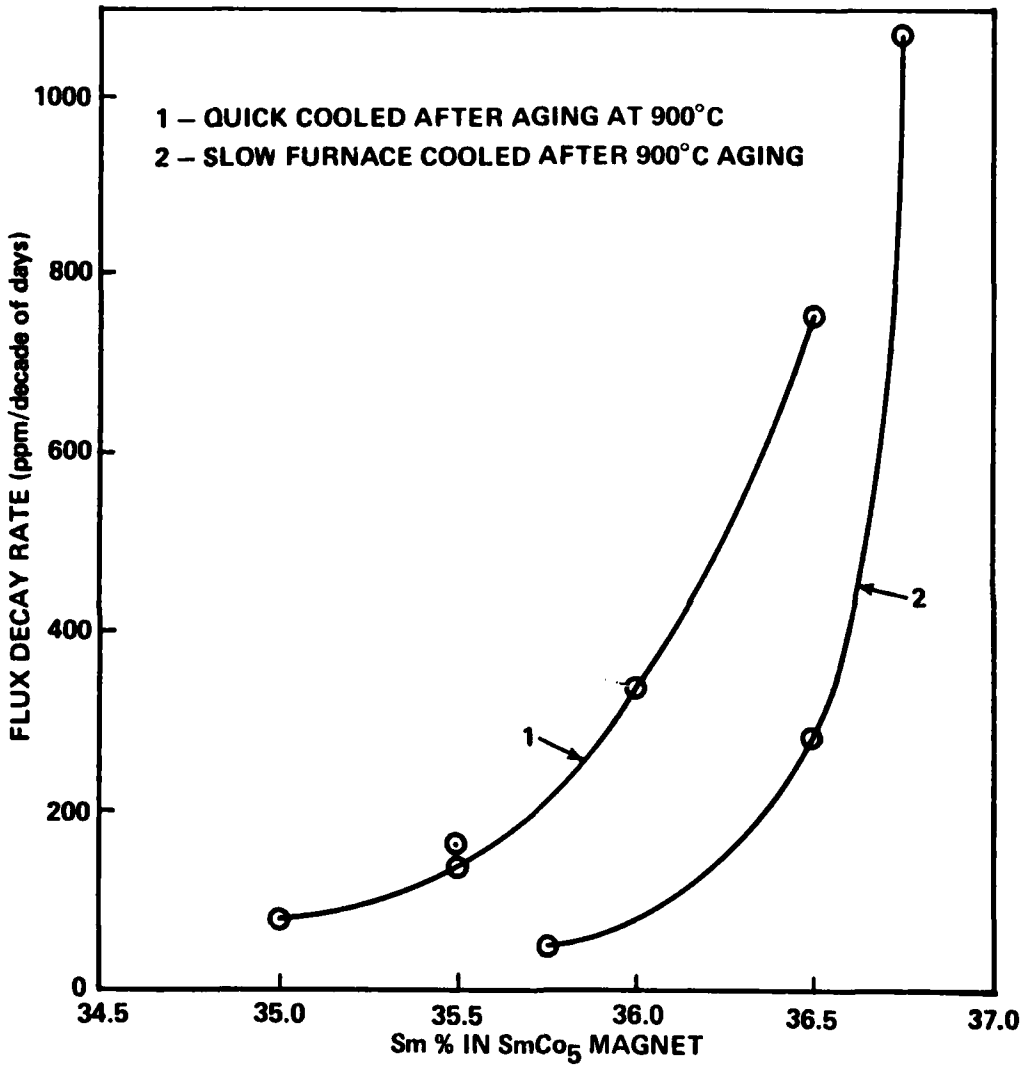

Figure 2. Flux decay rates of $SmCo_5$ magnets as a function of Sm content and thermal treatment.

3.1.1.3 Temperature Compensated and Thermally Compatible Magnets

Experimental work was also initiated on the development of temperature compensated magnets and the establishment of a correlation between thermal expansion measurements and energy product in $SmCo_5$ magnets.

Sinter experiments were performed to determine the compositions necessary to obtain zero temperature coefficients using $ErCo_5$ and $TbCo_5$ by replacing part of $SmCo_5$ with these materials. Larger percentages of these compounds were found to be necessary to obtain the zero temperature coefficient value than were expected on the basis of published data. As a result, the B_R values were appreciably lower than previously estimated. There was also some loss of B_R because of poor alignment that resulted from use of the die pressing and sintering fabrication procedure. The situation was somewhat alleviated by pursuing HIP processing instead of the conventional sinter technique. Initial HIPed magnets gave B_R values which were higher than those observed for the die-pressed/sintered magnets, but these lacked the necessary coercivity. However, based on the higher B_R values, the potential of higher energy product was seen if the coercivity could be improved by increasing the overall rare earth to cobalt ratio. Additional experiments performed with the Er-Sm-Co and Tb-Sm-Co ternary compositions for purposes of producing temperature compensated magnets resulted in maximum values of $(BH)_{max}$ of 11.6 MGOe and 9.0 MGOe respectively for these two alloy systems. Although these values were substantial improvements over what was previously accomplished, these were still lower than what was believed achievable.

The highest energy product $SmCo_5$ magnets prepared by HIP (21 MGOe) and sintering (18 MGOe) at CSDL were found to have two percent higher and two percent lower thermal expansion coefficients, respectively, than that of beryllium. An $SmCo_5$ magnet with an energy product of between 19 and 20 MGOe was, therefore, expected to give a very satisfactory match with beryllium for thermal expansion compatibility. This effort, as a result, appeared not to require much further investigation.

3.1.1.4 Radially oriented Full-Circle Ring Magnets

Radially oriented, full-circle $SmCo_5$ ring magnets have been impossible to produce by sinter technology, although many applications require such magnets. Using the HIP technique developed for $SmCo_5$ magnets at CSDL, ring magnets with radial orientation and high magnetic properties were produced within a well controlled geometry. These were expected to play an important role in the magnetic circuitry of torque generators in inertial instruments. Magnets of specified geometries were fabricated and found extremely useful in applications that included a low-cost gyroscope and a travelling wave tube. Superior performance was realized in both instances by using this product.

3.1.2 Sm-Co Magnets by Arc Plasma Spraying

3.1.2.1 Introduction

As discussed earlier, the motivation behind this effort was the considerable success achieved earlier with the $SmCo_5$ composition where the largest ever-to-be-measured room temperature coercivity value of 67.5 kOe was attained.[5] The energy product of the early sprayed $SmCo_5$ magnets, however, was limited to about 9 MGOe, mainly because these magnets were close-to-isotropic in structure. To obtain a higher level of flux from the sprayed magnets, one therefore needed to either introduce texture in the deposits or shift the material composition toward higher cobalt content (by the spraying of Sm_2Co_{17}-type deposits).

The approach that was initially taken was to attempt to produce Sm_2Co_{17}-type magnets with reasonably high coercivities. It was hoped that this would permit the fabrication of close-to-isotropic sprayed magnets with energy products of roughly 12 MGOe in a manner similar to the 9 MGOe value that was achieved with the $SmCo_5$ composition. Experiments performed toward this end showed that even though somewhat higher coercivities (higher than what are observed for sintered materials) were achievable in the sprayed samples, the improvements were

not significant and that the second quadrant characteristics remained poor.[27] The highest value for the maximum energy product that was measured in these sprayed Sm_2Co_{17}-type compositions was 6.6 MGOe. Therefore, it appeared that to attain energy products well in excess of the 7 to 9 MGOe that were achieved earlier for $SmCo_5$ compositions, it was important to produce crystallographically aligned deposits (of the $SmCo_5$ or the Sm_2Co_{17}-type stoichiometries) with the unique C-axis, which is also the easy axis of magnetization, preferably oriented in a direction perpendicular to the plane of deposition. Substantial efforts were, therefore, subsequently expended at attempting to produce aligned deposits using a variety of techniques with preliminary encouraging results.

3.1.2.2 Deposition Studies

Five starting powder compositions, in the range of 26.0 to 34.0 weight percent samarium, were selected and sprayed on water cooled copper substrates inside an inert gas environment plasma spray chamber. It was expected that the compositions of the deposited materials would be close to Sm_2Co_{17} with deposit compositions on either side of stoichiometry. X-ray diffraction patterns were obtained on several of the deposits with copper radiation and a diffracted beam graphite monochromator. Considerable broadening of the x-ray peaks was observed for all of the deposits. The diffuse patterns obtained on these materials were believed to be indicative of amorphous structures similar to what are conventionally obtained by rapid quenching techniques.

Several low temperature treatments were employed for optimizing the magnetic properites of the deposited materials. The maximum value of coercivity was measured as 7.9 kOe on a sample produced using the starting powder composition of 34.0 weight percent samarium. The other magnetic properties measured for this sample were B_R = 6500 G, H_c = 4050 Oe, and $(BH)_{Max}$ = 6.6 MGOe. These studies showed that grain size played a strong role in determining the value of H_{ci} in these binary Sm_2Co_{17}-type compositions. The improvements in the magnetic properties

from the low temperature treatments were attributed to increased homogenization and grain growth through crystallization related processes.

A few minor crystalline x-ray peaks were observed superimposed on an otherwise amorphous pattern in several of the deposits. In one sample, however, a single, sharp, crystalline peak was found superimposed on an otherwise amorphous-type pattern. A single peak was interpreted as illustrative of texture in the crystalline component of the deposit. The composition of the deposit, as measured by the x-ray fluorescence technique, was indicated to be about 30.0 weight percent samarium (which is in the two-phase $SmCo_5$ - Sm_2Co_{17} region of the phase diagram). The sole crystalline peak observed was found to be located at the (00.6) peak position for Sm_2Co_{17} - the compound of interest. This observation suggested that if proper cooling conditions were maintained at the substrate it might be possible to produce crystallographically aligned Sm_2Co_{17} materials by plasma spraying. Additional deposits formed with the aim of duplicating this observation were not successful.

Most of the deposits formed subsequent to the above efforts appeared to be more crystalline than the previous deposits. Additional cooling of the the substrate through the use of liquid-nitrogen-chilled helium gas also did not appreciably alter this situation. The x-ray peaks were still very broad, indicating that the grain size was extremely small. These deposits were fabricated with starting powder compositions of 42.0, 34.5, and 28.3 weight percent samarium resulting in deposit compositions corresponding closely to the $SmCo_5$, two-phase $SmCo_5$ + Sm_2Co_{17}, and Sm_2Co_{17} stoichiometries. Samples from all of these deposits were subjected to low temperature exposures to hydrogen gas. It was determined that the hydriding process resulted in a removal of the low level of crystallinity that existed in the as-sprayed condition. It was therefore decided to use the hydrogen-treated as well as the as-sprayed material for studies relating to inducing crystal orientation in the deposit.

3.1.2.3 Alignment Studies

Some initial experiments towards achieving alignment were performed with as-sprayed and hydrogen-treated samples by exposing them to a large (80 kOe) dc magnetic field at MIT's Francis Bitter National Magnet Laboratory. The magnetic field was applied during the process of crystallization and grain growth which occurs at temperatures of about 500°C in these compositions. These experiments indicated that whereas a marginal improvement had probably occurred in the sample produced from the 42.0 weight percent samarium alloy powder, the other two samples suffered deterioration in properties. It was concluded that additional experiments needed to be performed before firm conclusions could be reached with respect to the effect of applied magnetic fields on influencing alignment in the crystallized deposit.

Most of the subsequent work with plasma-sprayed Sm-Co alloys also concentrated on producing material with crystal anisotropy. A transmission electron microscopic (TEM) examination of the sample that had shown a single sharp crystalline x-ray peak located at the expected peak position for the (00.6) reflection from Sm_2Co_{17} showed the presence of large (unmelted) 1- to 10-μm particles, fine 50Å grains, and amorphous regions. It was concluded that the statistical sampling required for identifying the crystallites, responsible for the (00.6) x-ray peak, would require extensive effort. With respect to producing textured plasma sprayed alloys, the additional techniques examined included annealing the near-amorphous (fine grained and hydrogen treated) materials in the presence of large applied static magnetic fields and thermal gradients, and alloy deposition on substrates maintained at elevated temperatures. Experiments showed that magnetic field annealing did not induce texture in the material. Efforts on temperature gradient annealing also did not yield encouraging results. Depositions of $SmCo_5$ compositions at elevated temperatures, however, provided for deposits that were highly textured with the C-axis oriented perpendicular to the plane of deposition as indicated by x-ray diffraction patterns obtained on these materials. This was considered a

major breakthrough in the fabrication technology of these materials. Plasma spraying is a lower cost process and because of its near-net shape and size capability is expected to find many applications. Further efforts were expected to concentrate on optimizing the composition and heat treatments of the textured deposits for producing high quality $SmCo_5$ magnets.

3.2 Additional Work

3.2.1 $SmCo_5$ Magnets by Hot Isostatic Pressing

3.2.1.1 Flux Stability

As Figure 2 clearly indicated, a strong trend toward higher stability magnets was observed with the lowering of the nominal samarium content in the magnet. Since the stoichiometric $SmCo_5$ composition corresponds to approximately 34 weight percent samarium, the observed effect suggested that magnets with truly single phase 1-5 composition would be substantially superior (by a few orders of magnitude) to production Sm-Co magnets. (Production magnets exhibit flux decay rates of 1000 to 2000 ppm/decade time.) Conventional sintering requires the use of nominal concentrations well in excess of the 34 weight percent samarium stoichiometry for densification of the compact at sinter temperatures. The excess samarium is needed both for offsetting the samarium losses associated with oxygen pick-up during powder comminution in air and for providing the necessary liquid phase required for sintering to take place. It is, therefore, not possible to produce $SmCo_5$ magnets with compositions very close to stoichiometry using conventional sintering.

Hot isostatic pressing (HIP) was earlier demonstrated to be capable of providing the means for producing fully dense $SmCo_5$ magnets with starting compositions even lower than 35 weight percent samarium. As with previous experiments, additional nominal starting composition blends were made (with starting alloys of 34.5 and 41.8 weight percent

samarium) to yield compositions of 34.75, 35, and 35.25 weight percent samarium. Compacts were formed by cold isostatic pressing of aligned powders. The aligned compacts were hot isostatically pressed in a manner similar to that described in previous reports. The magnets were homogenized at elevated temperature and this was followed by an additional thermal optimization treatment at 900°C. The heat treated magnets were cooled from the 900°C temperature using both slow (furnace) as well as quick cooling procedures.

Table 1 provides the measured magnetic properties for these samples. Typical as-HIPed microstructures observed for these materials are shown in Figure 3. The maximum value of the remanence measured for this series of samples was 8.7 kG. In the majority of samples, the measured value of the coercivity was very poor. This result was directly correlatable to the high amount of the samarium-poor, Sm_2Co_{17} phase (that was observed as lightly etched areas) present in the microstructures. This Sm_2Co_{17} phase was made more visible and found to be dispersed in the form of particles after high temperature treatment of these materials (see Figure 4). Analysis performed on the comminuted powders revealed an oxygen content of 0.36 weight percent in the 35.25 weight percent samarium material and a considerably higher content in the other two blends (0.44 and 0.55). The effects of the samarium loss on coercivity and second quadrant demagnetization characteritics were quite deleterious (as was also suggested by the microstructural observations). Further plans to perform stability experiments were, therefore, abandoned.

It is clear that in order to achieve additional significant improvements in stability, attempts need to be made at producing near stoichiometric $SmCo_5$ magnets. This can be achieved by combining the advantages associated with the HIP technique with low oxygen processing of high purity starting alloy materials. Low oxygen processing of Sm-Co magnets has been demonstrated as feasible and has been pursued at CSDL under another program.

Table 1. Magnetic properties of 34.75, 35.0, 35.25 samarium content samples.

%Sm	Heat Treatment	B_R(kG)	H_{ci}(kOe)	H_c(kOe)	H_k(kOe)	$(BH)_{max}$(MGOe)
34.75	1	8.2	2.0			
34.75	2	8.9	2.3			
34.75	3	8.9	2.5			
34.75	4	8.9	3.7			
35.0	1	8.4	4.5	3.5	2.7	13.4
35.0	2	8.4	0.7			
35.0	3	8.2	7.7	4.1	3.5	14.0
35.0	4	8.9	4.0			
35.25	1	8.7	27.5	6.5	3.5	15.1
35.25	2	8.9	7.5	5.0	2.9	14.7
35.25	3	8.3	28.0	7.5	7.2	15.2
35.25	4	8.9	3.5			

1: 1075°C for 76 hrs, 900°C for 21 hrs, then quick cooled

2: 1075°C for 76 hrs, 900°C for 21 hrs, then furnace cooled

3: 1050°C for 76 hrs, 900°C for 21 hrs, then quick cooled

4: 1075°C for 90 hrs, then quick cooled

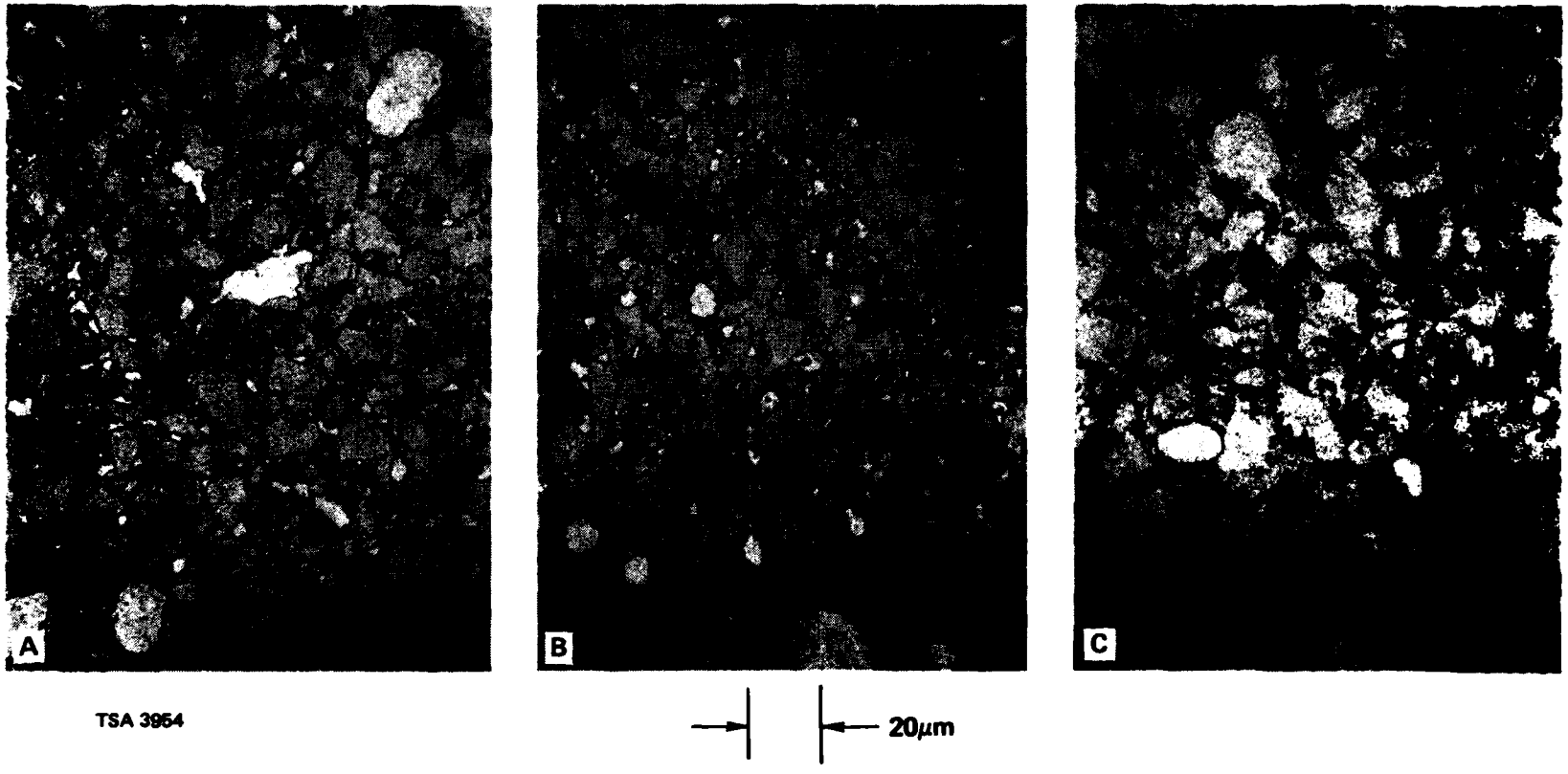

Figure 3. As-HIPed microstructures of (A) 36.75, (B) 35.0, and (C) 35.25 weight percent samarium samples.

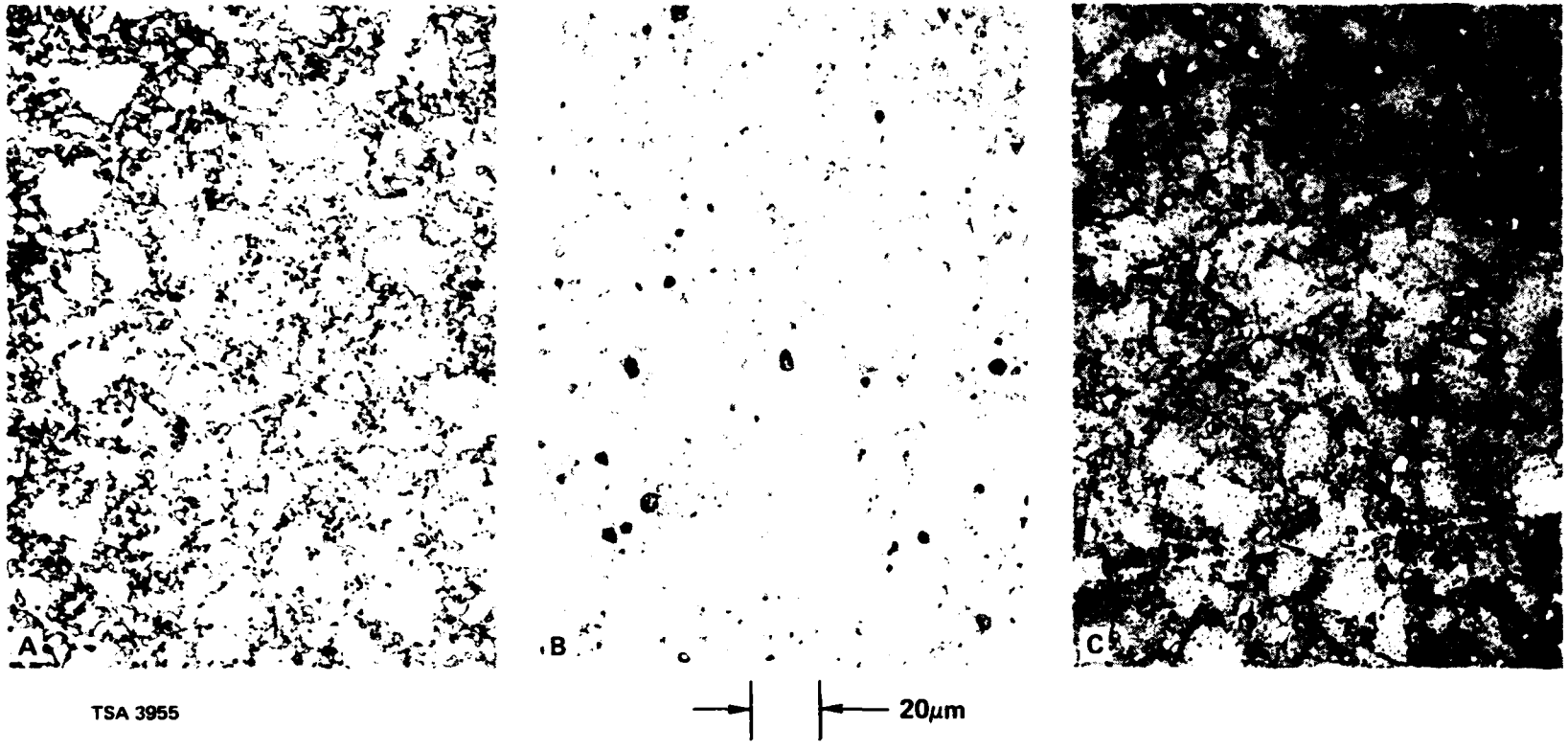

Figure 4. Microstructures after 1075°C, 76-hr and 900°C, 21-hr quick cool heat treatments.

3.2.1.2 Temperature Compensation

Efforts in this area concentrated on improving the processing of terbium and erbium substituted $SmCo_5$ magnets. Temperature-compensated magnets containing nominal blends of 35 and 40 weight percent $ErCo_5$ (65 and 60 weight percent $SmCo_5$ respectively) and 30 weight percent $TbCo_5$ (70 weight percent $SmCo_5$) were made using HIP. Previous attempts with such magnets had shown poor alignment and this had resulted in lower remanence and lower energy product than was believed possible with the selected compositions. The latest set of samples produced were not better in this regard. The microstructures from these samples are shown in Figure 5. The best properties obtained are listed in Table 2.

Table 2. Best magnetic properties obtained from recent batch of temperature compensated magnets [best is defined as the highest $(BH)_{max}$].

Composition	B_R (kG)	H_{ci} (kOe)	H_c (kOe)	H_k (kOe)	$(BH)_{max}$ (MGOe)
35 wt % erbium	6.9	19.5	6.0	3.5	9.9
40 wt % erbium	6.2	18.3	5.0	3.3	8.5
30 wt % terbium	6.5	19.0	6.3	13.0	9.7

All magnets were heat treated at 1140°C for 3 hrs, 900°C for 21 hrs, then quick cooled.

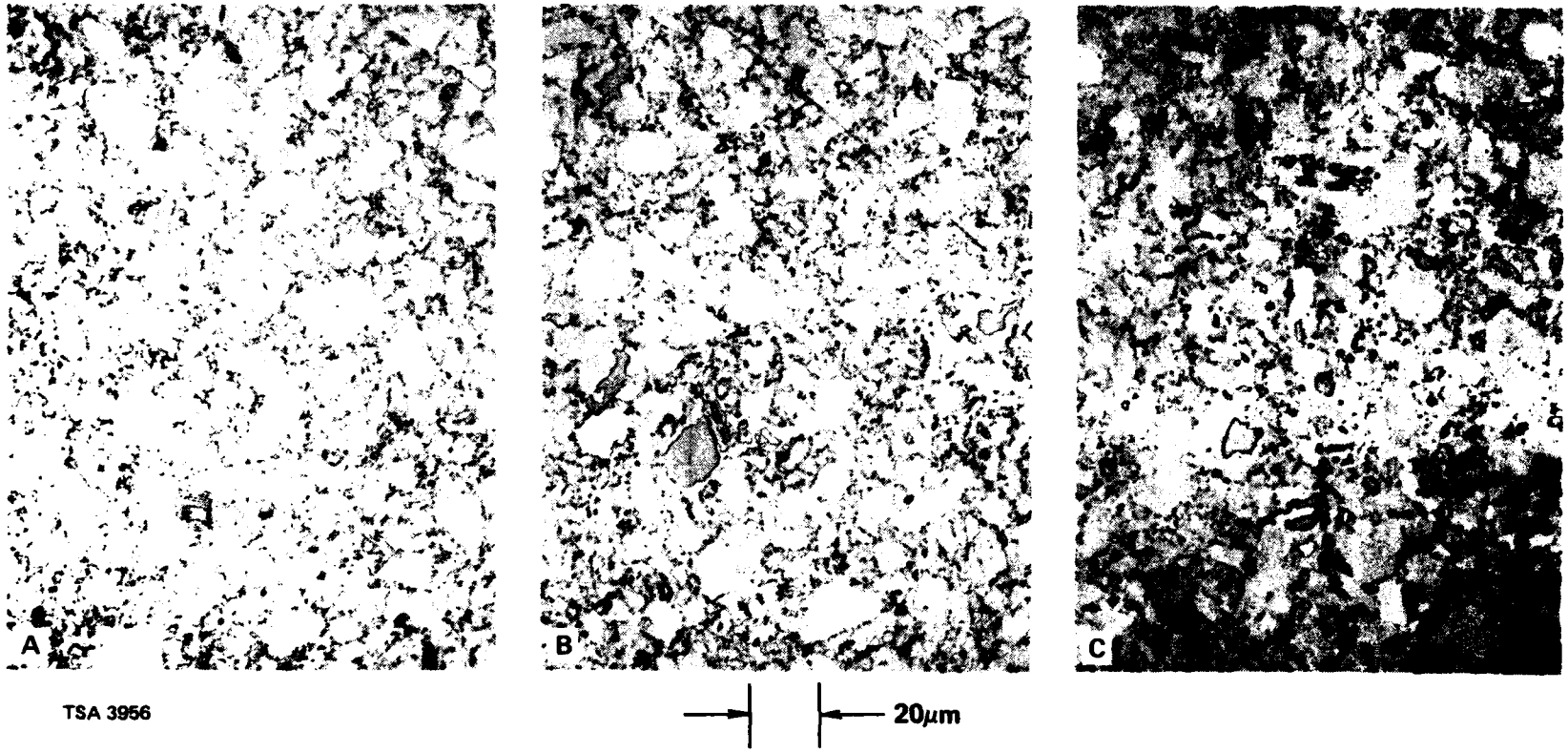

Figure 5. As-HIPed microstructure of temperature compensated samples.

Measurements of the temperature coefficient of the magnetic flux were made using the apparatus described in a previous report.[27] These data were found lacking with respect to reproducibility at the high level of accuracy (±2 to 5 ppm/°F) that was required to adequately determine a zero value for the temperature coefficient of magnetization. The temperature range over which data was collected was 70 to 150°F. The best values were obtained with the erbium substituted samples; the coefficients were on the order of +40 to -50 ppm/°F. The data suggested that the true zero value of the temperature coefficient of magnetization would occur at somewhat less than 35 weight percent substitution of $SmCo_5$ with $ErCo_5$.

For a more accurate determination of the level of compensation, from the device point of view, the 35 weight percent $ErCo_5$ sample was machined into 12 rectangular specimens. These were mounted onto a metal ring to simulate the magnet assembly in a gyro torquer. This assembly was then mounted into a temperature controlled test fixture with a drive motor which rotated the assembly at a constant speed of 500 rpm. With the assembly spinning, an AC voltage (Eo) was generated from the torquer coil; Eo was proportional to the assembly's air gap flux density. The value of Eo was monitored accurately as the temperature was changed 5 to 10°F from the normal operating temperature of 140°F. In this way the temperature sensitivity of the magnet assembly was determined.

The value of the temperature coefficient determined in this manner was found to be +5 ppm/°F over the range of 130 to 150°F. Only one such test was performed; however, the low value of the coefficient was encouraging.

3.2.2 Sm-Co Magnets by Arc Plasma Spraying

Most of the recent efforts at plasma spraying Sm-Co compositions were concentrated on producing aligned deposits with the aim of being able to fabricate sprayed magnets having high energy products. As reported previously, initial experiments had shown the feasibility of

producing aligned deposits of the $SmCo_5$ composition. This was confirmed by x-ray diffraction observations on a few deposits fabricated on steel substrates, which were maintained at high temperatures.

The technique consisted of achieving high substrate temperatures by heating up the substrate with the incident plasma flame (before alloy depositions were performed). The substrates consisted of low carbon steel bolt-shaped samples of different length which were mounted onto a water-cooled feedthrough located inside the plasma-spray chamber. Heat conduction from the surface was therefore directly influenced by the length of the substrate (over which the heat was conducted) and this resulted in the achievement of a variety of substrate temperatures. The temperature of the substrate was determined with a thermocouple attached to it while it was stationary and exposed to the plasma flame. Once the equilibrium temperature was measured, the thermocouple was disconnected and the substrate allowed to rotate. It was heated again for the predetermined period of time needed to allow equilibration of the temperature, and the depositions were performed by introducing the alloy powder into the plasma flame. As stated earlier, these efforts resulted in generating C-axis alignment in the $SmCo_5$ deposit compositions. Further efforts concentrated on attempting similar alignment in Sm_2Co_{17}-type deposits, through similar experimentation, as well as producing $SmCo_5$ magnets with energy product values higher than hitherto achieved.

3.2.2.1 Depositions of Sm_2Co_{17} Compositions

Several deposits were fabricated at substrate temperatures in the range of 550 to 1021°C. A starting alloy powder nominal composition of 28.3 percent samarium (the balance cobalt) was used for most of these deposits. Selection of this composition was based on past experience with the spraying of Sm-Co alloys which had shown a roughly 3 percent samarium loss to evaporation and oxidation. Figure 6 shows the x-ray diffraction patterns obtained on two of these deposits. One was deposited with a substrate temperature of about 570°C and the other with

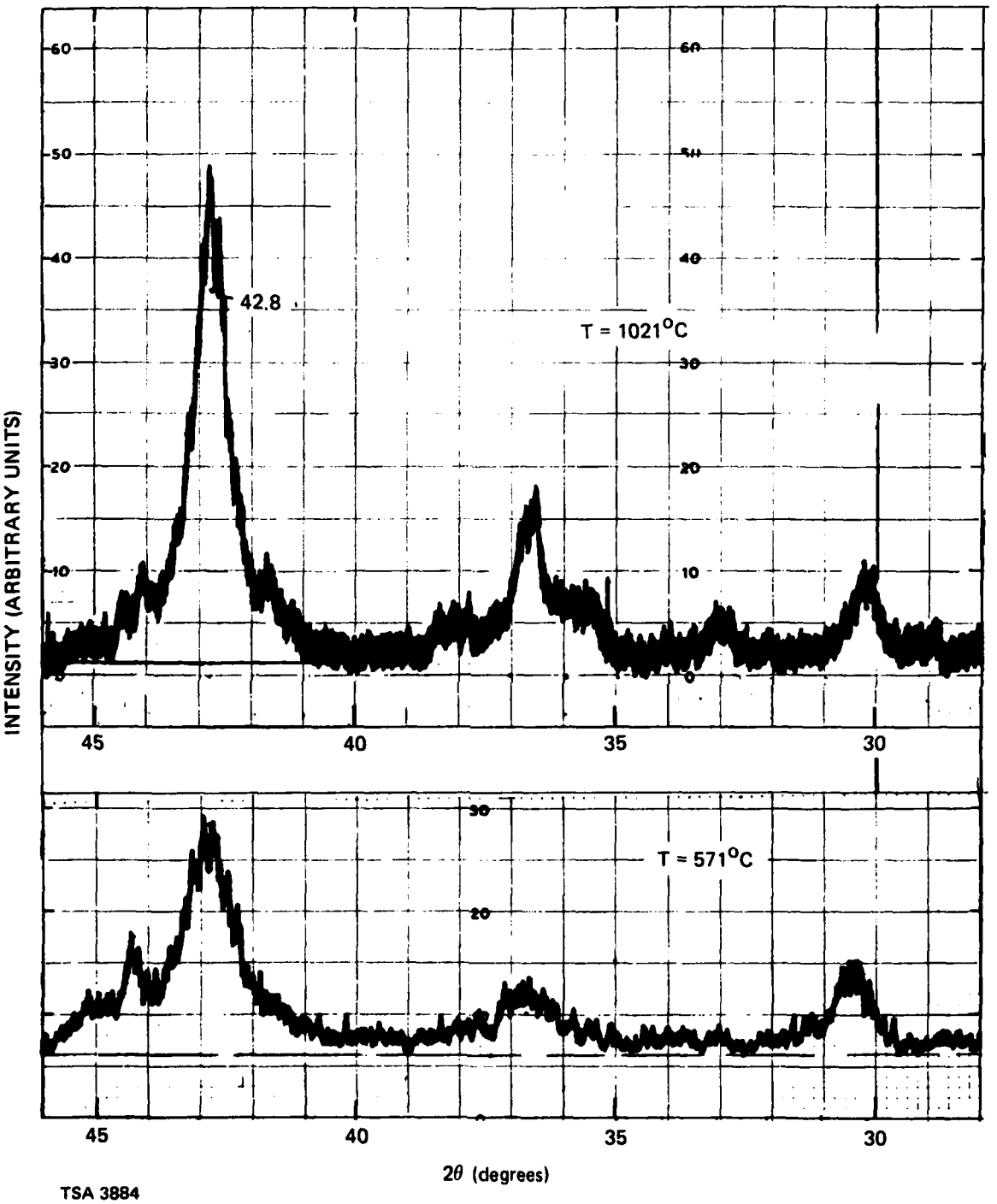

Figure 6. X-ray diffraction patterns from deposits formed with 28.3 wt % Sm powder at the substrate temperatures indicated. $Cu_{k\alpha}$ radiation.

a temperature of about 1020°C. Aside from a reduced x-ray line broadening of the peaks and more definition in the x-ray diffraction pattern, the effect of increasing temperature appeared negligible. The domain pattern from the 1020°C substrate temperature sample, as observed using the Kerr magneto-optic effect with polarized light, also supported the lack of a crystallographic texture in this sample.

These experiments indicated that it would be difficult to induce alignment in the Sm_2Co_{17} deposits using this procedure (unlike the situation with the $SmCo_5$ compositions, where the effects were more immediate and considerably more pronounced). Given the fact that meaningful levels of coercivity in the 2-17 compositions have only been achieved after pursuing complex thermal treatment procedures of 2-17 magnets containing additional elements such as copper, iron, zirconium, titanium, and hafnium, it was decided to concentrate further efforts on developing the properties of the $SmCo_5$ deposits.

3.2.2.2 Sprayed $SmCo_5$ Magnets Development

Preliminary work reported earlier had demonstrated the feasibility of achieving C-axis alignment in deposits of this composition. Additional efforts were therefore directed at developing high energy product $SmCo_5$ sprayed permanent magnets from such deposits. The work entailed examining variations in deposit composition and deposition conditions with the aim of producing magnets with acceptably high values of loop squareness and intrinsic coercivity. The deposited materials were examined for microstructure and domain contrast before, and after, a variety of thermal optimization treatments, using the techniques of (normal incidence) light and polarized light microscopy. Magnetic measurements were also performed on several of the samples.

X-ray patterns shown as Figure 28 in Reference 29 had demonstrated the strong influence of high substrate temperatures in inducing C-axis alignment in the deposit along the direction of deposition (which is normal to the plane of the deposit). The deposit fabricated at the highest substrate temperature of 1021°C in that series of samples had shown the best degree of alignment. Here too, however, some contributions were picked up from the (10.1) reflection indicating something less than perfect alignment. This figure is reproduced in this report as Figure 7. This situation was improved upon by performing the deposition at a still higher temperature of about 1127°C. The x-ray diffraction pattern obtained from such a deposit is shown in Figure 8, where the only peak observed was that from the (00.2) reflection. This indicated extremely good alignment in the deposit.

Even though good alignment was demonstrated as both feasible and achievable using these procedures, difficulties arose in not being able to produce magnets with good second quadrant characteristics, principally as they related to loop squareness and the intrinsic coercivity. Regions that etched to a lighter contrast then the matrix were observed in several of the as-sprayed deposits. These were samarium-depleted regions, probably consisting of the Sm_2Co_{17} phase. Presence of lightly etched Sm_2Co_{17} regions in $SmCo_5$ magnets are known to significantly impact upon the second quadrant characteristics.[20] Upon thermally treating the as-sprayed materials at temperatures in the range of 1000 to 1100°C (followed by an additional 900°C exposure) and quenching, large regions where the Sm_2Co_{17} phase had coalesced were made visible after metallographic polishing and etching of the samples. The excess Sm_2Co_{17} observed in deposits fabricated at high substrate temperatures was believed to have resulted from excessive samarium evaporation, from the Sm-Co alloy particles, during the deposition process. The higher the deposition temperature, the bigger was the loss in samarium and, therefore, the larger was the observed Sm_2Co_{17} precipitation. In addition to the foregoing, samples fabricated at the highest substrate temperatures also possessed very large grain sizes; possibly, as a result, leading to an additional reduction in coercivity and loop squareness.

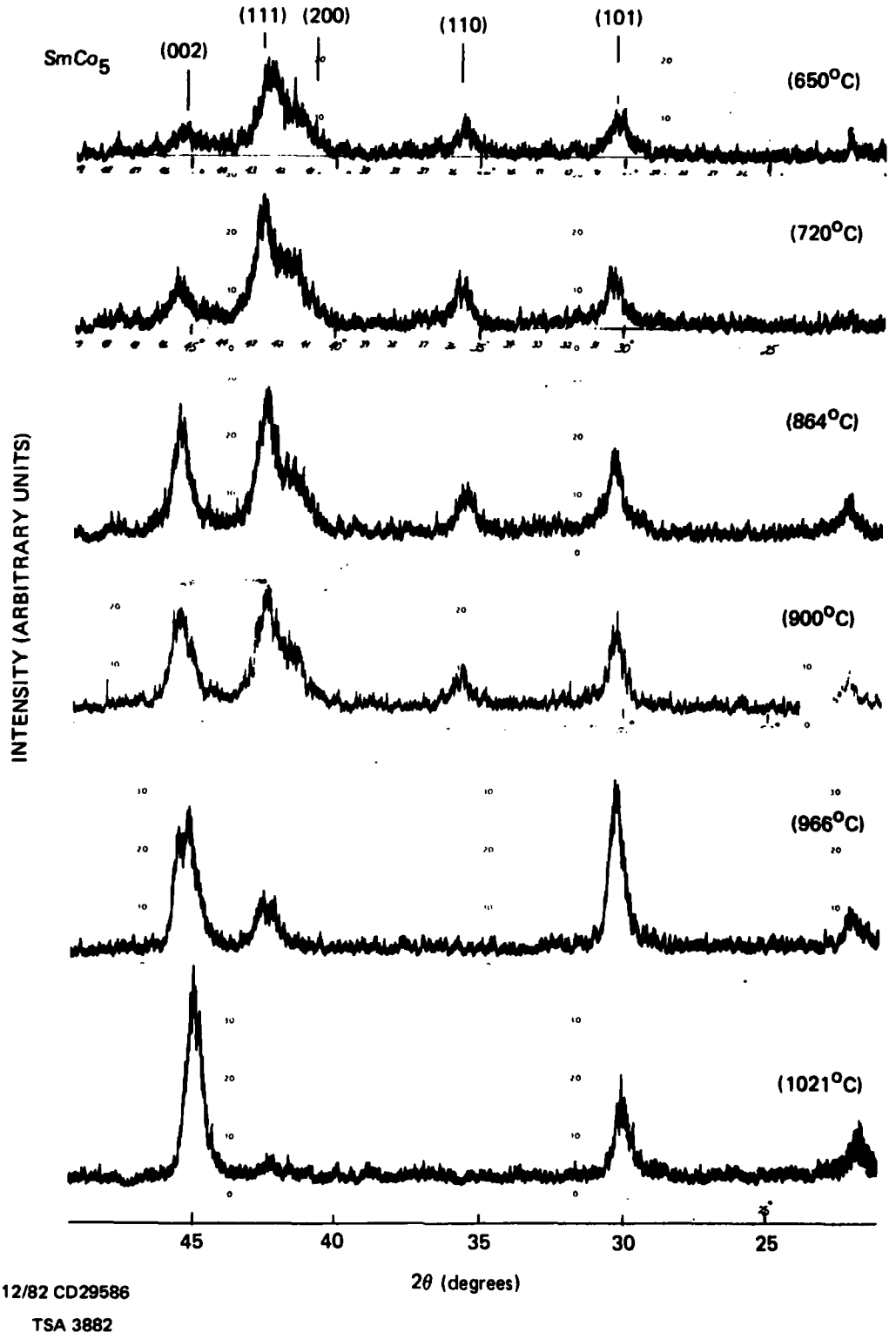

Figure 7. Effect of substrate temperature on alignment in sprayed SmCo deposits.

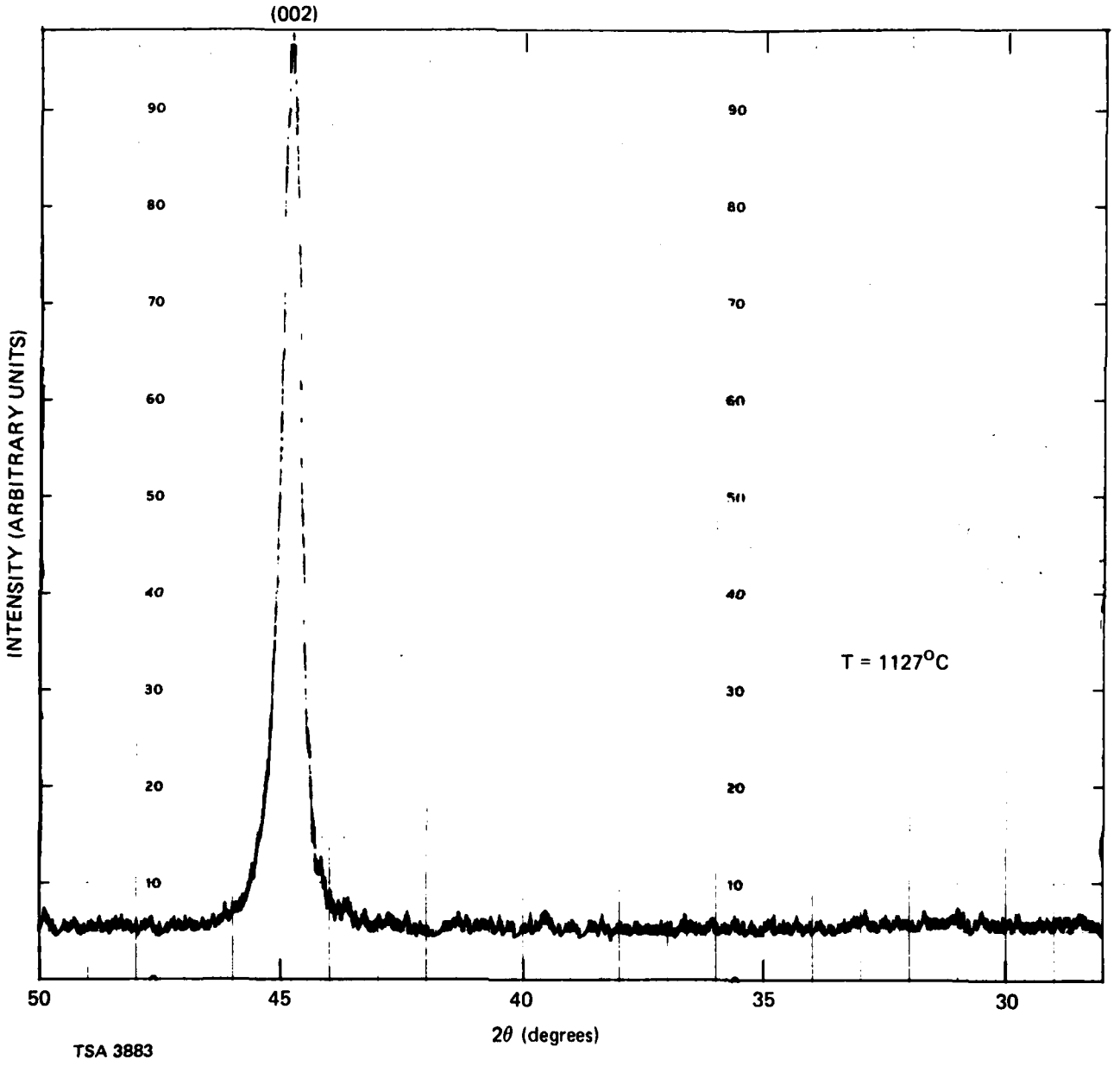

Figure 8. X-ray diffraction pattern from $SmCo_5$ deposit showing nearly perfect alignment.

Therefore, it was clear that a happy medium had to be reached between the competing processes of excessive grain growth combined with large samarium losses (from evaporation) on the one hand and good alignment on the other. The former consideration dictated material depositions at low substrate temperatures and the latter suggested the use of high temperatures. Success was partly achieved by modifying the powder feed nozzle geometry aimed at influencing the melting and plasma flame residence-time characteristics of the alloy powder particles. This resulted in the fabrication of a few deposits that showed extremely good alignment at the substrate temperature of about 1020°C. Figure 9(A) shows the C-axis pattern of such a deposit. Unfortunately, as shown in Figure 9(B), the samarium losses were still quite large. Figure 9(B) was obtained from a post-sprayed thermally treated sample of a deposit where the deposition conditions were similar (except for a larger powder feed rate) to the sample in Figure 9(A). It should be noted, however, that some variability in deposit quality was observed from run to run, apparently because of the nature of the process as it was practiced. Better controls on the various deposition parameters and substrate conditions should result in improved repeatability. The level of repeatability, however, appeared adequate for purposes of this research investigation. Instead of expensive, time-consuming corrections to the equipment, therefore, efforts were concentrated on actual experimentation.

Because of a lack of success at obtaining good alignment at temperatures lower than about 1020°C, it was decided to explore other ways of reducing the evaporation losses from these materials. The approach initially taken was to form deposits with alloy powders that possessed a coarser size distribution than was used for the earlier work. It was hoped that because of lower expected samarium losses from the surface of the coarser powder particles (because of low surface area-to-volume ratios that exist for the coarser particles), it might be possible to form well-aligned deposits at the lower temperature of about 1020°C while cutting down the samarium losses appreciably to influence retention of high coercivity and loop squareness. While this seemed to

(A) DOMAIN PATTERN- POLARIZED LIGHT

TSA 3878

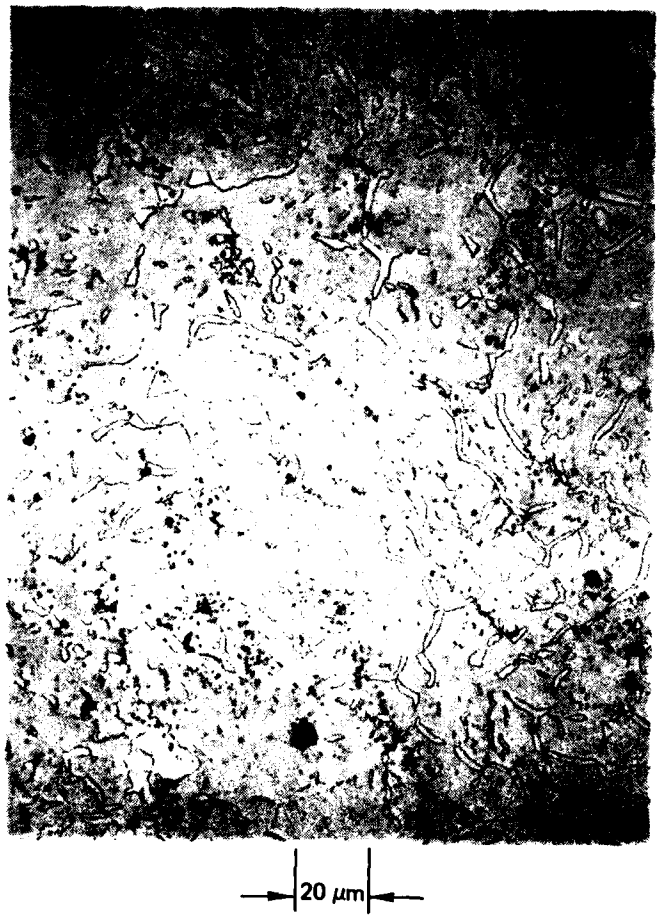

(B) 1100°C, 3 hours + 900°C, 24 hours, QC
SAMPLE SHOWING EXTENSIVE Sm_2Co_{17} PRECIPITATION

Figure 9. Micrographs of sprayed deposits (viewed along spray direction).

result in reducing the extent of the samarium loss, the surface generally appeared with a somewhat grainy structure where the domain patterns were not as well defined. Subsequent magnetic evaluations showed that the degree of alignment in these deposits was quite poor in contrast to deposits fabricated earlier with powder containing the finer particle sizes. Polarized light micrographs from two such deposits are shown in Figure 10. It is to be noted that the grain sizes are smaller in these micrographs compared to what was observed for the deposits made with the finer powders (see Figure 9). The grain size in Figure 9 can be inferred from the distribution of the (lightly etched) Sm_2Co_{17} phase which almost always occurs at the grain boundaries.

Alternative procedures were subsequently adopted to correct for the offset in composition arising from the evaporation-related losses. Attempts were made to spray uniformly homogeneous alloys containing higher levels of samarium. Because the amount of second phase observed in the microstructure indicated that an additional 2 to 4 percent samarium in the alloy would lead to near-elimination of the second (Sm_2Co_{17}) phase, alloy powders which had higher levels of samarium were sprayed. This procedure, however, even though it appeared to correct for the alloy composition, resulted in deposits that did not show good alignment.

At this point it appeared that the alloy composition had a strong bearing on the potential of being able to produce aligned deposits. Therefore, it was decided to pursue additional work with the alloy composition that had proved successful at achieving crystallographic texture. This approach included modifying the composition of the alloy powder (and, thus, the deposit) by blending it with a samarium-rich alloy. This was pursued initially by using a 46 weight percent samarium alloy for samarium enrichment. Figure 11 shows that a fair amount of success was achieved in a deposit produced by following this procedure. A few areas of a light etching phase were nevertheless observed in the matrix in addition to a few dark etching (Sm_2Co_7) regions. Very fine scale precipitation of the Sm_2Co_{17} phase was observed. The domain pattern observed for the as-polished sample is shown for this sample in Figure 12. It is clear that substantial partial success was achieved, both in the areas of

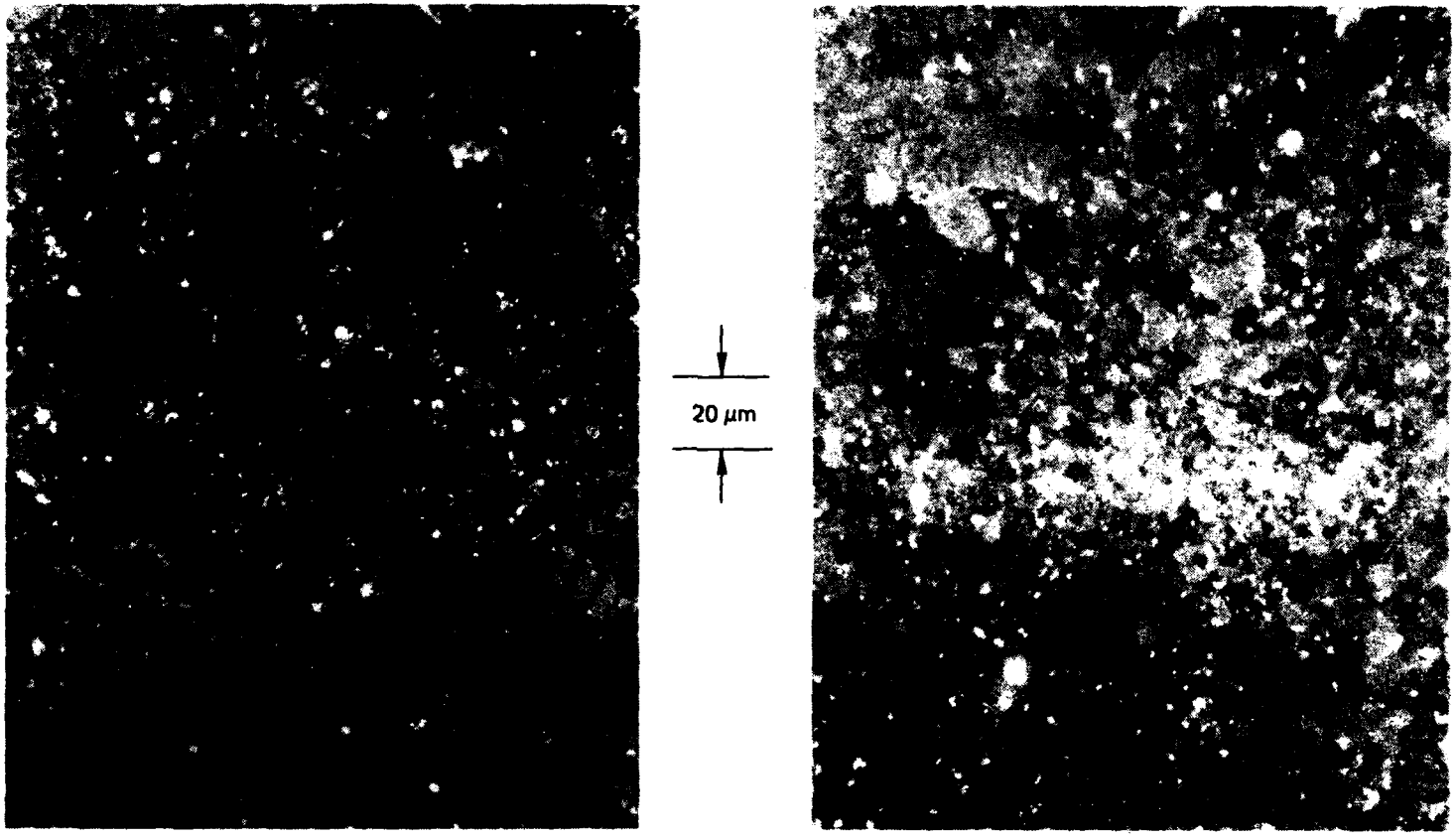

Figure 10. Polarized light domain contrast in deposits formed from coarser powder at the substrate temperatures indicated.

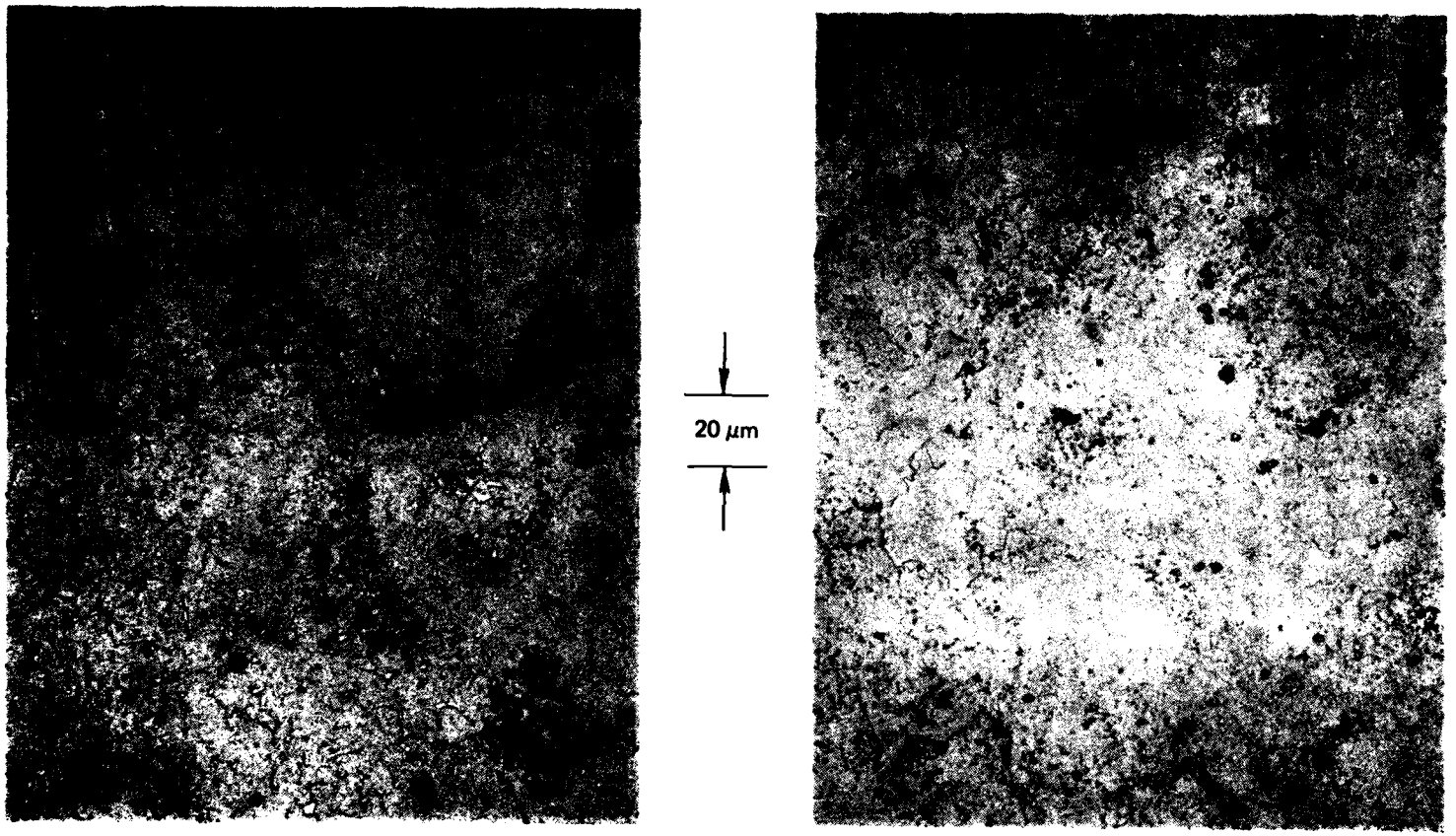

Figure 11. Micrographs of two regions observed in deposit made from Sm-rich blend of powders containing 46 wt % Sm alloy addition. After 1100°C, 3 hour + 900°C, 21 hour, quick cool thermal treatment.

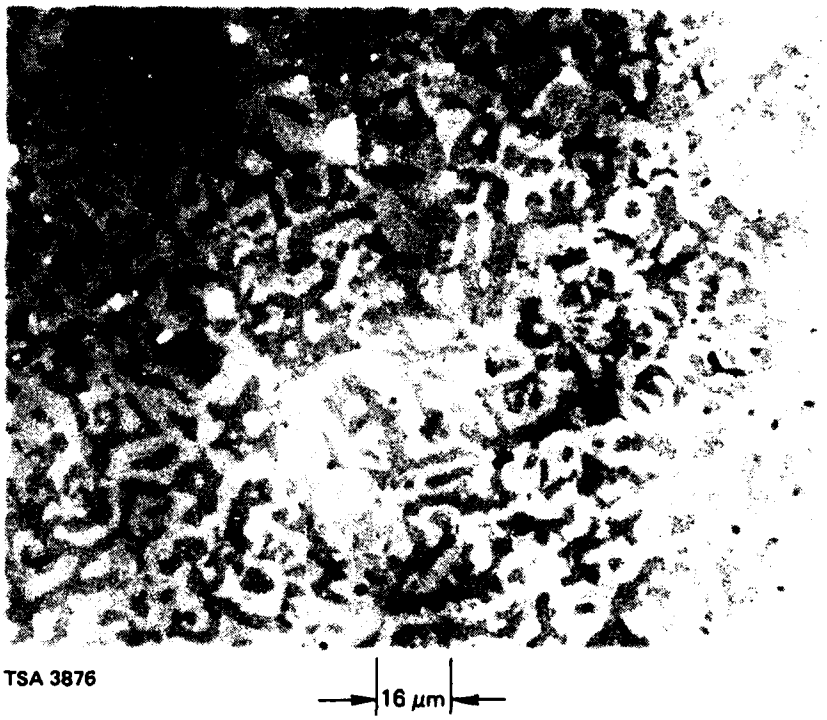

Figure 12. Polarized light micrograph showing domain contrast in sample with heat treated microstructure of Figure 11.

alignment as well as second phase reduction/elimination, by using these procedures.

The partial successes noted above were obtained, as stated previously, by enriching the alloy powder with the 46 weight percent samarium alloy. In light of the fact that problems were encountered in terms of achieving good alignment with the uniformly homogeneous samarium-rich alloy powder, it was decided that to improve the alignment of the deposits even more (than achievable with powder blends containing the 46 weight percent samarium alloy) it would be beneficial to enrich the samarium content by employing an even richer-in-samarium alloy. Powder blends containing 60 weight percent samarium alloy additions were therefore investigated. Because such an approach entailed an additional reduction in the volume percent of the samarium-enriching powder, it was hoped that it would also have a minimal effect on the alignment while effecting the needed correction to the composition of the deposited material. Mixed results were obtained in the several deposits that were formed. Areas of both good and poor alignment were observed as shown in Figure 13. The heat treated microstructure observed for this deposit as well as that for a similarly fabricated deposit are shown in Figure 14. While the former showed an absence of the second phase, the latter showed a fair amount of Sm_2Co_{17} precipitation. The former, however, contained a very large as-deposited grain size and had defects that appeared as cracks. The coercivity of this deposit was quite poor, possibly due to the very large grain size, and, therefore, good magnetic properties were not obtained from this material.

The next logical step was to increase the powder particle size of the 60 weight percent samarium alloy. Because the richer-in-samarium alloys melt at lower temperatures, there are more suspected evaporation losses from the higher-samarium-containing alloy powders for a given particle size. It was hoped that by selecting a powder which contained the 60 weight percent samarium alloy in coarser particle sizes, these losses could be substantially diminished. A few deposits were fabricated near the end of the program. These were yet to be evaluated for their properties and microstructure.

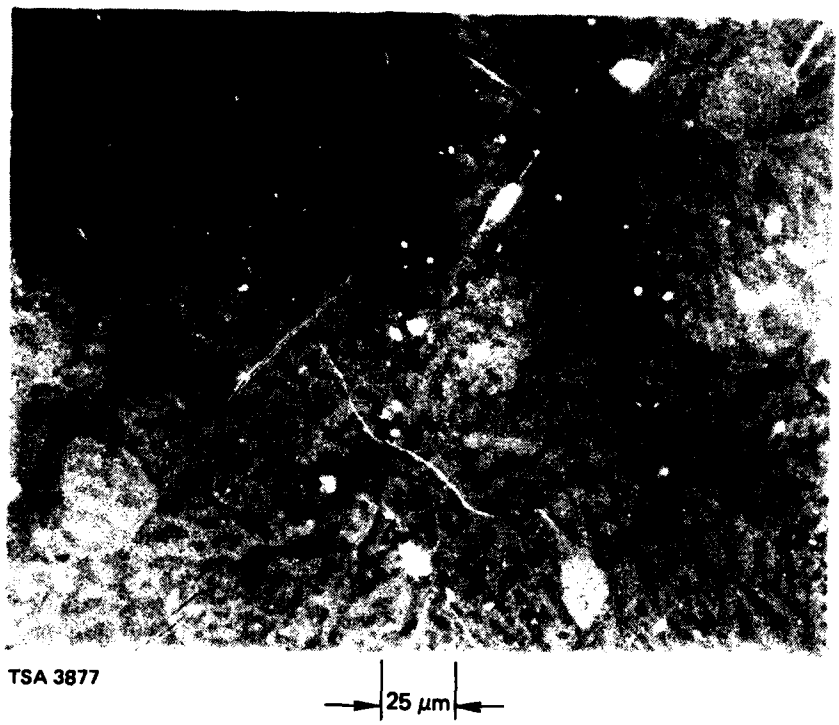

Figure 13. Domain structure of deposit formed with blend containing 60 wt % Sm powder.

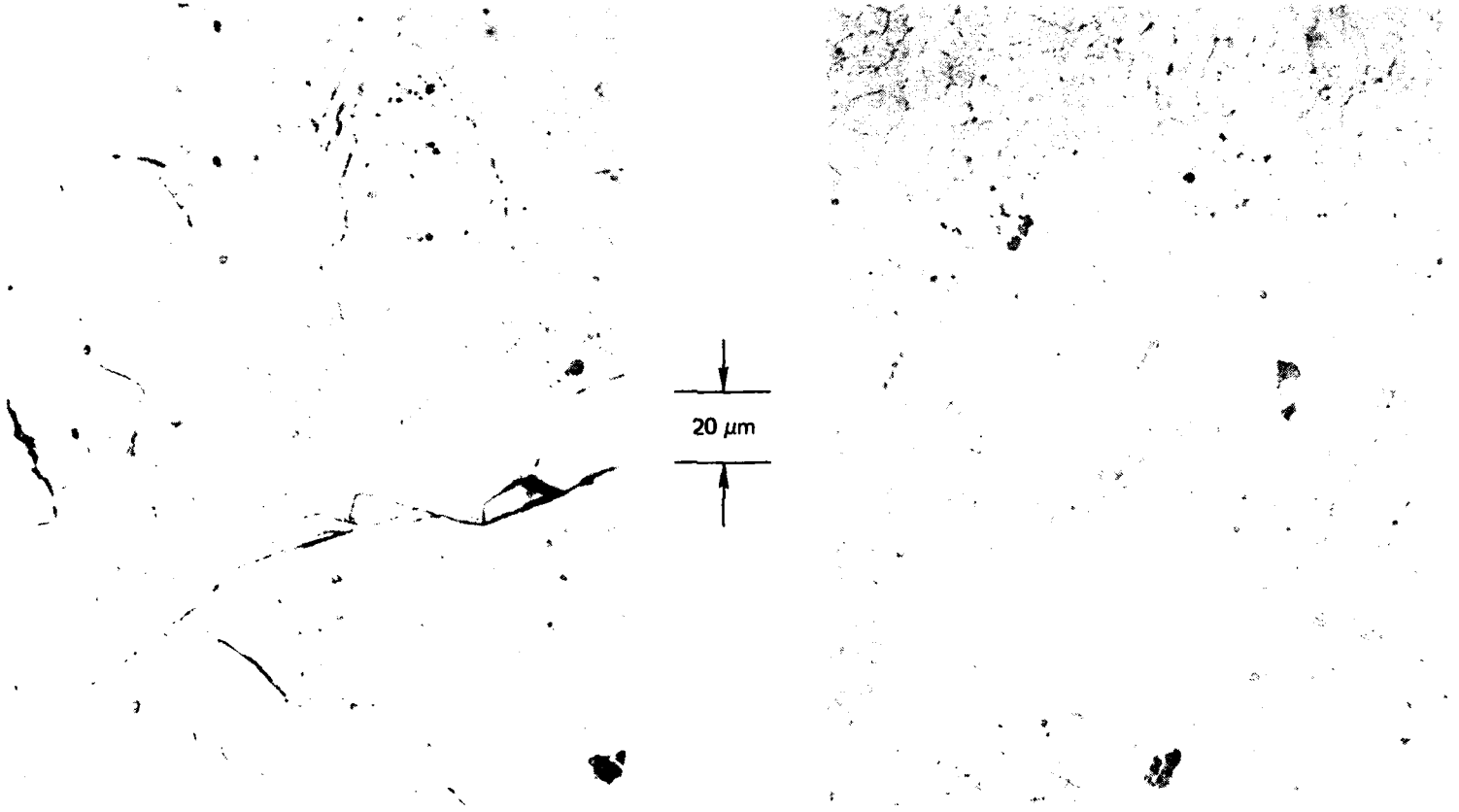

(A) 1075°C, 76 hours + 900°C, 21 hours, QC

(B) 1100°C, 3 hours + 900°C, 21 hours, QC

TSA 3881

Figure 14. Deposits fabricated similarly from powder blends with 60 wt % Sm alloy after indicated thermal treatments. 3% Nital etch.

3.2.2.3 Magnetic Properties

Magnetic characteristics as indicated by the saturation magnetization and second quadrant $4\pi M$ versus H loop behavior were, in general, routinely evaluated for deposits that appeared to have promise. Of the many deposits formed during this work, only a few came close to having properties that fell into this category. The magnet with the best combination of properties measured during this program had B_R = 7500G, H_{ci} = 13 kOe, $(BH)_{max}$ = 9.3 MGOe. The highest value of coercivity measured during this part of the work was 20 kOe.

SECTION 4

SUMMARY OF SIGNIFICANT RESULTS

A large number of significant findings resulted from the work performed under this program. Most of the original program objectives were met. Some highlights are briefly noted below.

(1) The conventional sintering process was sufficiently improved to yield aligned $SmCo_5$ magnets with record values of H_{ci} = 50 kOe and H_k = 33 kOe.

(2) Hot isostatic pressing (HIP) technology was introduced and developed for fabricating improved quality magnets.

(3) Use of HIP permitted the fabrication of full-circle radially oriented ring magnets. These were successfully applied to new designs of gyroscopes and travelling wave tubes.

(4) Studies were performed to determine thermal expansion match of the magnet to beryllium. It was found that little sarcrifice in properties was required to achieve good thermal expansion compatibility.

(5) Work aimed at determining the causes of flux instability in $SmCo_5$ magnets provided for such an understanding as well as the recipe needed to produce high flux stability magnets.

(6) Fabrication of temperature compensated, HIP 1-5 magnets with near-zero reversible temperature coefficient of magnetization values was demonstrated as feasible.

(7) Efforts aimed at successfully depositing 1-5 material with the hexagonal C-axis normal to the plane of deposition proved rewarding. This removed the major obstacle of potentially producing high energy product $SmCo_5$ magnets by this procedure.

SECTION 5

RECOMMENDATIONS FOR FUTURE WORK

Based on the work performed under this program, the following should be pursued for maximum utilization of the materials and processes that were investigated.

(1) Optimization of composition, alignment, and thermal treatment for producing still higher energy product temperature compensated magnets.

(2) Demonstration of the feasibility of producing full-circle radial ring magnets from the temperature compensated compositions.

(3) Development of the understanding of the flux decay mechanism in the above magnets.

(4) Study of the thermal expansion compatibility considerations of such magnets.

(5) Further development of the plasma spray process for producing high energy product $SmCo_5$ magnets which combine high coercivity with high alignment.

LIST OF REFERENCES

1. "Fabricating High Stability Sintered Sm-Co Magnets," Materials Research for Advanced Inertial Instrumentation, CSDL Proposal No. 7-780A, 1977.

2. Livingston, J.D., and M.D. McConnel, "Domain Wall Energy in Co-RE Compounds," J. Appl. Phys., Vol. 43, No. 11, p. 4756, November 1972.

3. Das, D., and W. Harrold, "Characterization of Sm-Co TWT Magnets," IEEE Trans. Magn., Mag-7, No. 2, p. 281, June 1971.

4. Mildrum, H.F., and K.M.D. Wong, "Stability and Temperature Cycling Behavior of RE-Co Magnets," Proc. 2nd. International Workshop on RE-Co Permanent Magnets, p. 35, June 1976.

5. Kumar, K., D. Das, and E. Wettstein, "High Coercivity, Isotropic Plasma-Sprayed Sm-Co Magnets," J. Appl. Phys., Vol. 49, No. 3, Part II, p. 2052, March 1978.

6. Kumar, K., D. Das, and E. Wettstein, "Sm-Co Magnets Resistant to 750°C," IEEE Trans. Magn., Mag-14, No. 5, p. 788, 1978.

7. Bartlett, R.W., and P.J. Jorgensen, "Microstructural Changes in $SmCo_5$ Caused by Oxygen Sinter-Annealing and Thermal Aging," J. Less Common Metals, 37, p. 21, 1974.

8. Das, D.K., et al, "Manufacturing Methods for Samarium-Cobalt Magnets," AFML TR-71-151, August 1971.

9. Benz, M.G., and D.L. Martin, "Cobalt-Mischmetal-Samarium Permanent Magnet Alloys, Process and Properties," J. Appl. Phys., 42, p. 2786, 1971.

10. Das, D.K., "Influence of Sintering Temperature on Magnetic Properties of Samarium-Cobalt Magnets," IEEE Trans. Magn., Mag-7, p. 432, September 1971.

11. Becker, J.J., "Rare Earth Compound Permanent Magnets," J. Appl. Phys., 41, p. 1005, 1970.

12. Becker, J.J., "Permanent Magnets Based on Materials with High Crystal Anisotropy," IEEE Trans. Magn., Mag-4, p. 239, September 1968.

13. Westendorp, F.F., "Nonaging Cold-Pressed $SmCo_5$ Magnets," IEEE Trans. Magn., Mag-6, p. 472, 1970.

14. Tatsumoto, E., et al, "Saturation Magnetic Moment ... High RCo_5," Jnl. de Physique, v. 32, p. CI-550, 1971 Supple.

15. Okamoto, T., et al, "Magnetic Moment and Easy Direction of Heavy Rare Earth Cobalt Compounds RCo_5," J. Phys. Soc., Japan, 34, p. 835, 1973.

16. Benz, M.G., R.P. Laforce, and D.L. Martin, "A Co-Gd-Sm Permanent Magnet with a Zero Temperature Coefficient," AIP Conf. Proc., No. 18, p. 1173, 1974.

17. Jones, F.G., and M. Tokunaga, "Low Temperature Coefficient Cobalt-Rare Earth Magnets," IEEE Trans., Magn., Mag-12, No. 6, p. 968, November 1976.

18. Kumar, K., D. Das, and C.R. Dauwalter (unpublished).

19. Strnat, K.J., and A.E. Ray, "Permanent Magnets Based on $R_2(Co, Fe)_{17}$ Phases: Their Potential and Present State of Development," Goldschmidt Informiert, 4/75, p. 47, 1975.

20. Kumar, K., and D. Das, "Magnetic Properties and Microstructures of Sprayed $SmCo_5$ Magnets Exposed to Intermediate Temperatures," J. Appl. Phys., 50(4), p. 2940, 1979.

21. Das, D., and K. Kumar, "New Technologies for Fabricating Improved Sm-Co Magnets", Proc. 3rd Int'l Workshop on RE-Co Magnets, p. 494, Dayton, Ohio, 1978.

22. Kumar, K., and D. Das, "Equilibrium and Metastable Samarium-Cobalt Deposits Produced by Arc Plasma Spraying", Thin Solid Films, 54(3), p. 263, 1978.

23. Kumar, K., D. Das, and R. Williams, "Role of Atmosphere in the Crystallization of Amorphous Plasma Sprayed Sm-Co Deposits", J. Appl. Phys., 51(2), p. 1031, 1981.

24. Das, D., "Twenty Million Energy Product Samarium-Cobalt Magnet", IEEE Trans. Magn., Mag-5(3), p. 214, 1969.

25. Das, D., E. Wettstein, and K. Kumar, Materials Research for Advanced Inertial Instrumentation, Task 3: Rare Earth Magnetic Material Technology As Related to Gyro Torquers and Motors (Technical Report No. 1), Charles Stark Draper Laboratory Report R-1177, July 1978. Office of Naval Research Contract N00014-77-C-0388.

26. Das, D., K. Kumar, and E. Wettstein, Materials Research for Advanced Inertial Instrumentation, Task 3: Rare Earth Magnetic Material Technology as Related to Gyro Torquers and Motors (Technical Report No. 2), Charles Stark Draper Laboratory Report R-1306, October 1979. Office of Naval Research Contract N00014-77-C-0388.

27. Das, D., K. Kumar, and E. Wettstein, Materials Research for Advanced Inertial Instrumentation, Task 3: Rare Earth Magnetic Material Technology as Related to Gyro Torquers and Motors (Technical Report No. 3), Charles Stark Draper Laboratory Report R-1435, December 1980. Office of Naval Research Contract N00014-77-C-0388.

28. Das, D., K. Kumar, and E. Wettstein, Materials Research for Advanced Inertial Instrumentation, Task 3: Rare Earth Magnetic Material Technology as Related to Gyro Torquers and Motors (Technical Report No. 4), Charles Stark Draper Laboratory Report R-1529, December 1981. Office of Naval Research Contract N00014-77-C-0388.

29. Das, D., E. Wettstein, and K. Kumar, Materials Research for Advanced Inertial Instrumentation, Task 3: Rare Earth Magnetic Material Technology as Related to Gyro Torquers and Motors (Technical Report No. 5), Charles Stark Draper Laboratory Report R-1614, December 1982. Office of Naval Research Contract N00014-77-C-0388.

30. Mildrum, H.F., and D.J. Iden, "Magnetic and Physical Properties of Commercially Available Rare Earth-Cobalt Permanent Magnets," Goldschmidt Informiert, 475, No. 35, p. 54, December 1975.

31. Das, D., K. Kumar, and C.R. Dauwalter, "Mechanism of Flux Decay in $SmCo_5$ Magnets," IEEE Trans. Magn., Mag-19, No. 5, p. 2050, September 1983.

BASIC DISTRIBUTION LIST

Organization	Copies
Defense Documentation Center Cameron Station Alexandria, VA 22314	12
Office of Naval Research Department of the Navy 800 N. Quincy Street Arlington, VA 22217	
ATTN: Code 471	1
Code 102	1
Code 470	1
Commanding Officer Office of Naval Research Branch Office Building 114, Section D 666 Summer Street Boston, MA 02210	1
Commanding Officer Office of Naval Research Branch Office 536 South Clark Street Chicago, IL 60605	1
Naval Research Laboratory Washington DC 20375	
Attn: Codes 6000	1
6100	1
6300	1
6400	1
2627	
Naval Air Development Center Code 302 Warminster, PA 18964 ATTN: Mr. F.S. Williams	1
Naval Postgraduate School Monterey, CA 93840 ATTN: Mechanical Engineering Department	1

Organization	Copies
Naval Air Propulsion Test Center Trenton, NJ 08628 ATTN: Library	1
Naval Construction Batallion Civil Engineering Laboratory Port Hueneme, CA 93043 ATTN: Materials Division	1
Naval Missile Center Materials Consultant Code 3312-1 Point Mugu, CA 92041	1
Commanding Officer Naval Surface Weapons Center White Oad Laboratory Silver Spring, MD 20910 ATTN; Library	1
David W. Taylor Naval Ship Research and Development Center Materials Department Annapolis, MD 21402	1
Naval Undersea Center San Diego, CA 92132 ATTN: Library	1
Naval Underwater System Center Newport, RI 02840 ATTN: Library	1
Naval Weapons Center China Lake, CA 93555 ATTN: Library	1

BASIC DISTRIBUTION LIST (Continued)

Organization	Copies
Naval Air Systems Command Washington, DC 20360 ATTN: Codes 52031 52032	
Naval Sea System Command Washington, DC 20362 ATTN: Code 035	1
Naval Facilities Engineering Command Alexandria, VA 22331 ATTN: Code 03	1
Scientific Advisor Commandant of the Marine Corps Washington, DC 20380 ATTN: Code AX	1
Naval Ship Engineering Center Department of the Navy Washington, DC 20360 ATTN: Code 6101	1
Army Research Office P.O. Box 12211 Triangle Part, NC 27709 ATTN: Metallurgy and Ceramics Program	1
Army Materials and Mechanics Research Center Watertown, MA 02172 ATTN: Research Programs Office	1
Air Force Office of Scientific Research Bldg. 410 Bolling Air Force Base Washington, DC 20332 ATTN: Chemical Science Directorate	1
Electronics & Solid State Sciences Directorate	1
NASA Headquarters Washington, DC 20546 ATTN: Code RRM	1
	1
NASA (216) 433-4000 Lewis Research Center 21000 Brookpark Road Cleveland, OH 44135 ATTN: Library	1
National Bureau of Standards Washington, DC 20234 ATTN: Metallurgy Division	1
Inorganic Materials Division	1
Director Applied Physics Laboratory University of Washington 1013 Northeast Fortieth Street Seattle, WA 98105	1
Defense Metals and Ceramics Information Center Battelle Memorial Institute 505 King Avenue Columbus, OH 43201	1
Metals and Ceramics Division Oak Ridge National Laboratory P.O. Box X Oak Ridge, TN 37380	1
Los Alamos Scientific Laboratory P.O. Box 1663 Los Alamos, NM 87544 ATTN: Report Librarian	1
Argonne National Laboratory Metallurgy Division P.O. Box 229 Lemont, IL 60439	1
Brookhaven National Laboratory Technical Information Division Upton, Long Island New York 11973 ATTN: Research Library	1

BASIC DISTRIBUTION LIST (Continued)

Organization	Copies	Organization	Copies
Library Building 50, Room 134 Lawrence Radiation Laboratory Berkeley, CA	1	Office of Naval Research Branch Office 1030 East Green Street Pasadena, CA 91106	1

SUPPLEMENTARY DISTRIBUTION LIST

Technical and Summary Reports

Professor Albert E. Miller
University of Notre Dame
Box 8
Notre Dame, IN 46556

Professor Karl J. Strnat
University of Dayton
Magnetic Laboratory
Dayton, OH 45469

Dr. J.J. Becker
General Electric Research
and Development Center
P.O. Box 8
Schenectady, NY 12301

Professor W.E. Wallace
Department of Chemistry
University of Pittsburgh
Pittsburgh, PA 15213

Dr. Richard P. Allen
Battelle-Northwest
Richland, WA 99352

Dr. Howard T. Savage
Naval Surface Weapons Center
White Oak
Silver Spring, MD 20910

Mr. Harold Garrett
Air Force Materials Laboratory
LTE, Bldg. 16
Wright-Patterson Air Force Base
Dayton, OH 45433

Dr. L.D. Jennings
Army Materials and Mechanics
Research Center
Watertown, MA 02172

Dr. J.O. Dimmock, Director
Electronic and Solid State
Sciences Program (Code 427)
Office of Naval Research
Arlington, VA 22217

Assistant Chief for Technology
(Code 2000)
Office of Naval Research
Arlington, VA 22217

Strategic Systems Projects Office
Department of the Navy
Washington, DC

Professor G.S. Ansell
Rensselaer Polytechnic Institute
Dept. of Metallurgical Engineering
Troy, NY 12181

Dr. David L. Martin
General Electric Research
and Development Center
P.O. Box 8
Schenectady, NY 12301

Professor M. Cohen
Massachusetts Institute of Technology
Department of Metallurgy
Cambridge, MA 02139

Professor J.W. Morris, Jr.
University of California
College of Engineering
Berkeley, CA 94720

Professor O.D. Sherby
Stanford University
Materials Sciences Division
Stanford, CA 94300

SUPPLEMENTARY DISTRIBUTION LIST (Continued)

Dr. E.A. Starke, Jr.
Georgia Institute of Technology
School of Chemical Engineering
Atlanta, GA 30332

Professor David Turnbull
Harvard University
Division of Engineering and
Applied Physics
Cambridge, MA 02139

Dr. D.P.H. Hasselman
Montana Energy and MHD Research
and Development Institute
P.O. Box 3809
Butte, MT 59701

Dr. L. Hench
University of Florida
Ceramics Division
Gainesville, FL 32601

Dr. J. Ritter
University of Massachusetts
Department of Mechanical
Engineering
Amherst, MA 01002

Professor J.B. Cohen
Northwestern University
Dept. of Material Sciences
Evanston, IL 60201

Director
Materials Sciences
Defense Advanced Research
Projects Agency
1400 Wilson Boulevard
Arlington, VA 22209

Professor H. Conrad
University of Kentucky
Materials Department
Lexington, KY 40506

Dr. A.G. Evans
Dept. of Material Sciences
and Engineering
University of California
Berkeley, CA 94720

Professor H. Herman
State University of New York
Material Sciences Division
Stony Brook, NY 11794

Professor J.P. Hirth
Ohio State University
Metallurgical Engineering
Columbus, OH 43210

Professor R.M. Latanision
Massachusetts Institute of Technology
77 Massachusetts Avenue
Room E19-702
Cambridge, MA 02139

Dr. Jeff Perkins
Naval Postgraduate School
Monterey, CA 93940

Dr. R.P. Wei
Lehigh University
Institute for Fracture and
Solid Mechanics
Bethlehem, PA 18015

Professor G. Sines
University of California
at Los Angeles
Los Angeles, CA 90024

Professor H.G.F. Wilsdorf
University of Virginia
Department of Materials Science
Charlottesville, VA 22903

Dr. A. Tauber
Dept. of the Army
HQ, U.S. Army Electronic Command
Fort Monmouth, NY 07703

SUPPLEMENTARY DISTRIBUTION LIST (Continued)

Mr. K.K. Jin
Strategic Systems Division
Autonetics Group
3370 Miraloma Avenue
P.O. Box 4192
Anaheim, CA 92803

Mr. N. Horowitz
The Aerospace Corporation
2350 East El Segundo Boulevard
El Segundo, CA

Mr. Francis W. Wessbecher
Unit Head
Inertial Component Engineering
Singer Kearfott Division
150 Totowa Road
Wayne, NJ 07470

National Magnet Laboratory
Massachusetts Institute of Technology
145 Albany Street
Cambridge, MA 02139
ATTN: Dr. Donald T. Stevenson (2)
Assistant Director

Mr. Carl Flom
Delco Electronics
7929 South Howell
Box 471
Milwaukee, WI 53201

David Schwab
Air Research Mfg. Co.
2525 W. 190th Street
Torrance, CA 90209

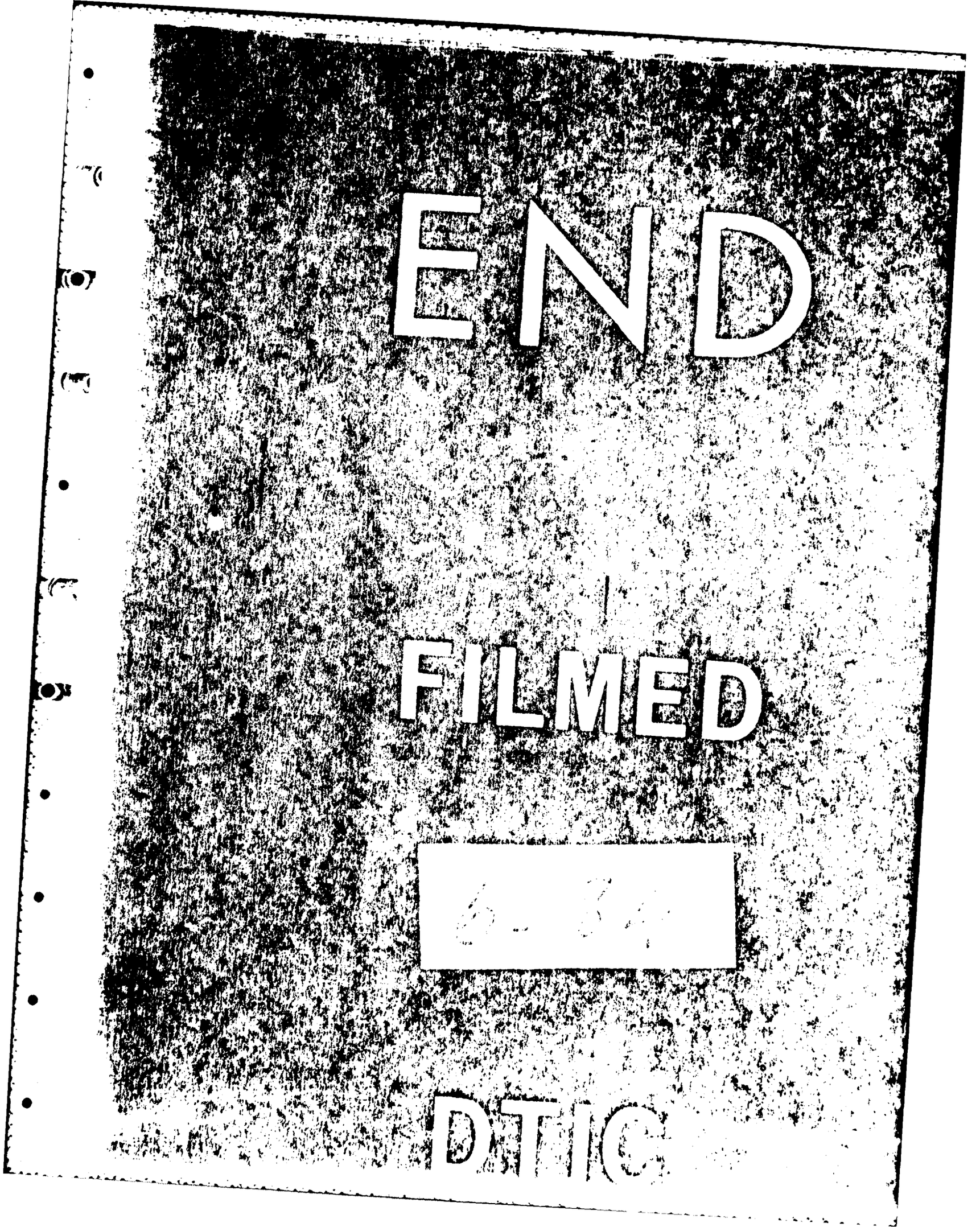
END
FILMED
DTIC